Clinical Science (2024) **138** 327–349
https://doi.org/10.1042/CS20230533

Research Article

Therapeutic implication of human placental extract to prevent liver cirrhosis in rats with metabolic dysfunction-associated steatohepatitis

Mitsuyoshi Yamagata[1], Mutsumi Tsuchishima[1], Takashi Saito[1], Mikihiro Tsutsumi[1,2] and Joseph George[1,2]

[1]Department of Hepatology, Kanazawa Medical University, Uchinada, Ishikawa 920-0293, Japan; [2]Center for Regenerative Medicine, Kanazawa Medical University Hospital, Uchinada, Ishikawa 920-0293, Japan

Correspondence: Joseph George (georgej@kanazawa-med.ac.jp)

Metabolic dysfunction-associated steatohepatitis (MASH) is always accompanied with hepatic fibrosis that could potentially progress to liver cirrhosis and hepatocellular carcinoma. Employing a rat model, we evaluated the role of human placental extract (HPE) to arrest the progression of hepatic fibrosis to cirrhosis in patients with MASH. SHRSP5/Dmcr rats were fed with a high-fat and high-cholesterol diet for 4 weeks and evaluated for the development of steatosis. The animals were divided into control and treated groups and received either saline or HPE (3.6 ml/kg body weight) subcutaneously thrice a week. A set of animals were killed at the end of 6th, 8th, and 12th weeks from the beginning of the experiment. Serum aspartate aminotransferase (AST), alanine aminotransferase (ALT), hepatic malondialdehyde (MDA), and glutathione content were measured. Immunohistochemical staining was performed for α-smooth muscle actin (α-SMA), 4-hydroxy-2-nonenal (4-HNE), collagen type I, and type III. Control rats depicted progression of liver fibrosis at 6 weeks, advanced fibrosis and bridging at 8 weeks, and cirrhosis at 12 weeks, which were significantly decreased in HPE-treated animals. Treatment with HPE maintained normal levels of MDA and glutathione in the liver. There was marked decrease in the staining intensity of α-SMA, 4-HNE, and collagen type I and type III in HPE treated rats compared with control animals. The results of the present study indicated that HPE treatment mediates immunotropic, anti-inflammatory, and antioxidant responses and attenuates hepatic fibrosis and early cirrhosis. HPE depicts therapeutic potential to arrest the progression of MASH towards cirrhosis.

Introduction

Metabolic dysfunction-associated steatotic liver disease (MASLD) is a clinicopathologic condition mostly associated with metabolic syndrome and a major health problem in developed nations [1,2]. It includes a spectrum of liver impairment ranging from inflammation to metabolic dysfunction-associated steatohepatitis (MASH), advanced fibrosis, and early cirrhosis [3,4]. Depends on the etiology and lifestyle, some cases may progress into liver cirrhosis and hepatocellular carcinoma (HCC), leading to death [5]. Metabolic syndrome and the associated insulin resistance, oxidative stress, lipid peroxidation, and proinflammatory cytokines have significant contributions in the development and progression of MASLD [6,7]. This is especially true in developed nations with more sedentary lifestyles, where the imbalance between caloric intake and caloric output steadily increases [8]. Since an increasing number of patients suffering from MASH are developing liver failure, liver transplantation is the only therapeutic option [9]. However, due to the shortage of organs available for transplant and the associated complications and rejection after transplantation, alternative treatment methods are highly necessary [10,11].

Received: 19 May 2023
Revised: 14 February 2024
Accepted: 21 February 2024

Accepted Manuscript online: 21 February 2024
Version of Record published: 05 March 2024

Clinical Science (2024) **138** 327–349
https://doi.org/10.1042/CS20230533

Table 1 Nutrient composition of Funabashi Farm SP and HFC diets

	SP diet	HFC diet
Diet composition (%)		
SP diet	100	68
Palm oil	–	25
Cholesterol	–	5
Cholic acid	–	2
Ingredients (%)		
Crude protein	20.8	14.1
Crude lipid	4.8	35.3
Crude fiber	3.2	2.2
Crude ash	5.0	3.4
Moisture	8.0	5.4
Carbohydrate	58.2	39.6

The total energy was 4.14 kcal/g in SP diet and 5.72 kcal/g in HFC diet.

Human placental extract (HPE) is a rich source of multipotent progenitor cells, several growth factors, and nutrients [12]. HPE exhibits many therapeutic properties and acts as a strong stimulant for tissue repair, immunomodulation, cell proliferation, and tissue regeneration [13,14]. Placental extracts have been utilized in a variety of clinical conditions, including liver function and wound healing, where the growth factors, amino acids, anti-inflammatory, and angiogenic agents have proven to be beneficial [15,16]. HPE is enriched in enzymes, nucleic acids, vitamins, amino acids, peptides, fatty acids, and minerals [17]. In addition, HPE is a potent source of natural antioxidants and free radical scavenging enzymes and may reduce oxidative stress in various pathological conditions [18,19]. The potential role of HPE in treating osteoarthritis and cartilage regenerative medicine has been recently evaluated [20]. Animal experimental studies on lipopolysaccharide stimulated proinflammatory cytokines and mediators demonstrated that HPE has strong anti-inflammatory and analgesic effects [21]. Since HPE has potent antioxidant substances, anti-inflammatory mediators, and growth factors, it could be used as a therapeutic agent to protect liver cells and also for regeneration of hepatocytes after chronic liver injury such as MASH and advanced fibrosis [22,23]. In the present study, we evaluated whether HPE can prevent the progression of simple steatosis to MASH, advanced fibrosis, and early cirrhosis in an experimental animal model. We employed SHRSP5/Dmcr rats that derived from a stroke-prone spontaneously hypertensive rat, which progresses to MASH and advanced fibrosis from simple steatosis on treatment with a high-fat and high-cholesterol (HFC) diet [24]. This animal model was further evaluated and demonstrated that feeding with HFC diet can develop hepatic lesions similar to those in human MASH pathology [25].

Materials and methods

Animals

About 6 weeks old SHRSP5/Dmcr male rats (body weight: 123.2 $\pm$ 5.1 g) were procured from the Disease Models Co-operative Research Association (DMCRA), Kyoto, Japan. All the animal experiments were carried out as per the Guide for the Care and Use of Laboratory Animals published by the US National Institutes of Health (NIH Publication No. 86-23, revised 1996). The protocol was also approved by the Animal Care and Research Committee of Kanazawa Medical University on the Ethics of Animal Experiments (# 2018-29). All the animal experiments were performed in accordance with the relevant guidelines and regulations. The animals were housed in stainless steel wire mesh cages in air-conditioned rooms with a relative humidity of 50 $\pm$ 10% and 10-15 air changes per hour. All the animals had automatic 12 h light/dark cycles and *ad libitum* access to food and water.

Experimental design

All the animal experiments were carried out in the animal house at Kanazawa Medical University, Japan. A total of 60 rats were used in the study. They were divided into 12 groups of 5 rats each and 7 groups were fed with HFC diet (Funabashi Farm, Chiba, Japan). The remaining five groups were fed with normal diet [Stroke-prone diet (SP diet), Funabashi Farm, Chiba, Japan] and treated as diet and HPE control. The nutrient composition of both SP diet and HFC diet is presented in Table 1. A group of five rats fed with HFC diet were killed at 4 weeks to evaluate the development of hepatic steatosis. Among the remaining six groups, three groups served as control and the other three

groups for HPE treatment. The control groups were injected subcutaneously with 0.36 ml/100 g body weight of saline three times per week, and the HPE groups were injected with 0.36 ml/100 g body weight of HPE (LAENNEC, Japan Bio Products, Tokyo, Japan) in the same way as the control. One group of five rats was sacrificed in both saline and HPE treated groups at the end of 6, 8, and 12 weeks, and the blood and livers were collected. A set of five rats fed with the SP diet were also sacrificed at 4th, 6th, 8th, and 12th weeks, along with the treated groups. The SP diet and HPE control group of five rats were injected with the same dose of HPE as above and killed at the end of the study. All the animals were anaesthetized with isoflurane before euthanasia, and blood was collected from the right jugular vein. The animals were euthanized under deep anesthesia using a rodent guillotine and excess blood was allowed to drain out. The surgical procedures were performed inside a clean bench in the adjacent room of the animal house. About 3 mm thick liver tissue was cut from the median lobe and instantly fixed in 10% phosphate-buffered formalin for histopathological studies. Another portion of the liver was frozen at −80°C for biochemical analyses. Animal body weight and liver wet weight were measured during the procedures. All methods reported are in accordance with the ARRIVE guidelines 2.0 for reporting *in vivo* experiments.

Measurement of aspartate aminotransferase and alanine aminotransferase in serum

Blood was allowed to clot at 37°C for 3–5 h and the serum was separated after centrifugation at 3000 rpm in a clinical centrifuge. Aspartate aminotransferase (AST) and alanine aminotransferase (ALT) present in the serum were measured using an auto-analyzer for animal samples. AST and ALT values are presented as International Units per liter (IU/liter) of serum.

Determination of malondialdehyde and glutathione in the liver tissue

Malondialdehyde (MDA) is a characteristic marker of lipid peroxidation and an indicator of elevated cellular oxidative stress [26]. Hepatic MDA content in the liver tissue was measured based on a fluorometric technique employing a MDA assay kit (Cat# NWK-MDA01, Northwest Life Science, Vancouver, WA, U.S.A.). Approximately 100 mg of frozen liver tissue was homogenized in 1 ml of ice-cold 50 mM Tris-HCl buffer (pH 8) containing 150 mM NaCl, 1 mM EDTA, and 1% Triton X-100. Then, 50 µl of the homogenate was treated with 150 µl of 5% 5-sulfosalicylic acid solution and vortexed well. It was allowed to stand on ice for 10 min and centrifuged at 12,000 × ***g*** for 10 min at 4°C. Hepatic MDA content was determined in the supernatant diluted 1:1 with distilled water. Hepatic MDA content is presented as nmoles/g wet liver tissue.

Reduced glutathione (GSH), a tripeptide (γ-glutamyl-cysteinyl-glycine), is the major free thiol in the biological system and the most potent scavenger of superoxide and free radicals. GSH content was measured in the liver tissue using 50 µl of the above supernatant (diluted to 100 µl with distilled water) and employing a glutathione assay kit (Cat# CS0260, Millipore-Sigma, St. Louis, U.S.A.). Hepatic GSH content is presented as µmoles/g wet liver tissue.

Histopathological evaluation of the liver tissue

The extent of the pathogeneses of MASH and the development of hepatic fibrosis and early cirrhosis were examined in the liver tissue during the course of the study. The formalin-fixed liver tissues were processed in a tissue processor optimized for liver tissue, embedded in paraffin blocks, and cut into sections of 5 µm thickness. The sections were stained with Hematoxylin and Eosin (H&E) to study histopathological changes and Azan trichrome to evaluate the deposition of collagen fibers in the liver tissue as per the standard protocol. The stained sections were examined with an Olympus BX53 microscope attached with a DP 71 digital camera (Olympus Corporation, Tokyo, Japan) and photographed. The histopathological evaluation and grading were performed by a pathologist who is unaware of the time points of the study and course of the treatment. The changes of pathological features during HFC diet administration and after the treatment with HPE were scored as per the method of Bedossa et al. [27] and are reported as SAF score (steatosis, activity [comprises hepatocyte ballooning and lobular inflammation], and fibrosis). The steatosis score (S) was assessed as the quantities of large or medium-sized lipid droplets, from 0 to 3 (S0: <5%; S1: 5–33%, mild; S2: 34–66%, moderate; S3: >67%, marked). Activity grade (A) was scored from 0 to 3 as A0 (no activity), A1 (mild activity), A2 (moderate activity), and A3 (severe activity). The stages of fibrosis (F) was assessed as follows: F0 (no fibrosis), F1 (portal and periportal fibrosis), F2 (bridging fibrosis), and F3 (advanced fibrosis and early cirrhosis). The average grade was calculated after examining 10 lobules on each liver section.

Clinical Science (2024) **138** 327–349
https://doi.org/10.1042/CS20230533

Table 2 Sequences of the Rattus norvegicus mRNA primers used in real-time RT-PCR

Transcript	Genebank Number	Primer sequence	Start	Stop	Length (mer)	Product size (bp)
α-SMA	BC158550	5′-GCTGCTCCAGCTATGTGTGA-3′ (F)	40	59	20	338
		5′-TCCGTTAGCAAGGTCGGATG-3′ (R)	377	358	20	
Collagen Type I (α1)	BC133728	5′-TGGTGAGACGTGGAAACCTG-3′ (F)	215	234	20	193
		5′-CTTGGGTCCCTCGACTCCTA-3′ (R)	407	388	20	
Collagen Type III (α1)	BC087039	5′-TGCAATGTGGGACCTGGTTT-3′ (F)	118	137	20	501
		5′-GATAGCCACCCATTCCTCCG-3′ (R)	618	599	20	
PCNA	BC060570	5′-CACGTATATGCCGGGACCTT-3′ (F)	581	600	20	235
		5′-GGAGACAGTGGAGTGGCTTT-3′ (R)	815	796	20	
GAPDH	AF106860	5′-TGTGAACGGATTTGGCCGTA-3′ (F)	864	883	20	208
		5′-GATGGTGATGGGTTTCCCGT-3′ (R)	1071	1052	20	

F: forward primer; R: reverse primer.

Immunohistochemical staining for α-smooth muscle actin, 4-hydroxy-2-nonenal, collagens type I, and type III

Activation and transformation of quiescent hepatic stellate cells into myofibroblast like cells with the expression of α-smooth muscle actin (α-SMA) is a characteristic feature for initiation of fibrosis [28]. Similarly, increased production of 4-hydroxy-2-nonenal (4-HNE) is a prominent marker of cellular oxidative stress and membrane lipid peroxidation [29]. The deposition of newly formed type I and type III collagen fibers in the hepatic parenchyma is a distinctive feature of hepatic fibrosis and early cirrhosis [30]. In order to obtain explicit information about the above parameters during the course of the study, we performed immunohistochemical staining for α-SMA, 4-HNE, and collagens type I and type III on formalin fixed paraffin liver sections. The deparaffinized and hydrated liver sections were blocked with a protein block (Cat# ab64226) for 30 min at room temperature to prevent non-specific binding. After washing thrice in cold phosphate-buffered saline (PBS), the liver sections were treated with primary antibodies against α-SMA (Cat# ab5694), type I collagen (Cat# ab34710), type III collagen (Cat# ab23445) (Abcam, Chuo-ku, Tokyo, Japan), and 4-HNE mouse monoclonal antibody (Cat# HNEJ-2, Nikken Seil, Shizuoka, Japan) separately, and incubated in a moisturized slide chamber (Evergreen Scientific, Los Angeles, CA, U.S.A.) at 4°C overnight. The sections were then washed 3–5 times in PBS and incubated with broadspectrum biotinylated secondary antibody for 2 h at room temperature. The slides were washed again with PBS, treated with streptavidin-peroxidase conjugate, and incubated for another 1 h at room temperature. The final stain was developed after treating the sections with 3% 3-amino-9-ethylcarbazole (AEC) in N, N-dimethylformamide for 5–10 min. The stained sections were washed and counterstained with Mayer's hematoxylin for 2 min, mounted using aqueous-based mounting medium, and dried on air. The slides were examined under a microscope (Olympus BX53, Tokyo, Japan) fixed with a digital camera (Olympus DP71) and captured multiple images in different magnifications. The staining intensity of 10 randomly selected microscopic fields was quantified using Image-Pro Discovery software (Media Cybernetics, Silver Spring, MD, U.S.A.).

Quantitative real-time PCR for markers of liver cirrhosis and hepatic regeneration

In order to monitor the expression of major molecular markers of liver cirrhosis and to evaluate the effect of HPE treatment on hepatic regeneration, we performed quantitative real-time PCR for the mRNA levels of α-SMA, collagen type I, collagen type III, and proliferating cell nuclear antigen (PCNA) in the liver tissue of rats administered with SP and HFC diet and treated with HPE at 12 weeks. Small pieces of liver tissue were flash frozen in liquid nitrogen and stored at −80°C. Total mRNA was isolated from the frozen liver tissue employing the PureLink RNA Mini Kit (Cat# 12183018A, Invitrogen, Carlsbad, CA, U.S.A.) in combination with Trizol (Cat# 15596026, Thermo Fisher, Waltham, MA, U.S.A.) as per the protocol. The gene-specific primers for rat α-SMA, collagen type I (α1 chain), collagen type III (α1 chain), PCNA, and GAPDH were designed using Primer-BLAST software (National Institutes of Health, Bethesda, MD). The details of Rattus norvegicus mRNA primer sets used for the study are provided in Table 2. The cDNA was synthesized with 1–2 μg of isolated total RNA using the PrimeScript 1st strand cDNA Synthesis Kit (Cat# 6110A, Takara Bio, Shiga, Japan) in a total volume of 20 μl in RNase-free dH_2O at 42°C for 60 min.

Real-time quantitative PCR (qPCR) was carried out with PowerTrack SYBR Green Master Mix (Cat# A46012, Thermo Fisher, Waltham, MA, U.S.A.) on ABI 7900HT Fast Real-Time PCR System (Applied Biosystems, Foster City, CA). The synthesized cDNA was diluted to 20 fold with RNase-DNase-free water. The qPCR reaction was carried out with 5 μl of diluted cDNA, 10 μl of PowerTrack SYBR Green Master Mix, nuclease free water containing gene specific primers, and the sample buffer in a total volume of 20 μl in a 384-well microplate. All the samples were processed in triplicates. The qPCR machine was run on standard cycling mode with the parameters set as enzyme activation at 95°C for 2 min (1 cycle), denature at 95°C for 15 s and anneal/extend at 60°C for 60 s (40 cycles). All the data were normalized to the GAPDH gene.

Data analysis and statistics

Statistical analysis was undertaken only for the data set where each group size was at least $n=5$. All declared group size is the number of independent values and all statistical analyses were done on the independent values. Outliers were not excluded from the data set. Arithmetic mean and standard deviation (SD) were calculated for all the data and presented as Mean $\pm$ SD. All the data were analyzed and compared either by using analysis of variance (ANOVA) or Student's *t*-test. A value of $P<0.05$ was considered statistically significant.

Results

Animal body weight and liver wet weight

The animal body weight and liver wet weight, as well as the liver wet weight to body weight ratio, are presented in Figure 1. There was no difference in body weight between control and HPE treated animals in both SP and HFC diet groups at any time point of the study (Figure 1A). The liver weight was significantly reduced at 8 and 12 W in HPE treated animals in the HFC diet group (Figure 1B). There was marked decrease of liver wet weight to body weight ratio at 6, 8, and 12 W in HPE treated animals in the HFC diet group (Figure 1C).

Serum levels of AST and ALT during the pathogenesis of MASH and hepatic cirrhosis and the effect of HPE treatment

The serum levels of AST and ALT during the pathogenesis of HFC diet induced MASH and hepatic cirrhosis in SHRSP5/Dmcr rats and the effect of HPE treatment are presented in Figure 2. Both AST and ALT levels are significantly increased at 6, 8, and 12 W compared with 4 W in rats fed with HFC diet ($^{\#}P<0.001$). Concurrent treatment with HPE resulted in a marked reduction of elevated AST and ALT levels in all the weeks studied except at the 6th week in the case of ALT. There was no difference between both AST and ALT levels in rats fed with the SP diet at 4 W compared with at any time point of the study. Similarly, there was no difference between both AST and ALT levels in rats fed with the SP diet at 12 W compared with the rats fed with the SP diet and treated with HPE.

Malondialdehyde and glutathione levels in the hepatic tissue of rats fed with HFC diet and the effect of HPE treatment

An increased level of malondialdehyde (MDA) is a potent marker of cellular oxidative stress and peroxidation of membrane lipids. The hepatic MDA levels in SHRSP5/Dmcr rats fed with the HFC diet and the effect of concurrent HPE treatment are presented in Figure 3A. MDA levels were markedly increased in the liver tissue of animals fed with HFC diet at 8 and 12 W compared with 4 W ($^{\#}P<0.001$). Simultaneous treatment with HPE resulted in restoration of normal levels of MDA on all the weeks studied. The mean hepatic MDA level was not significantly different at 6 W in rats treated with HFC diet compared with HFC diet with HPE. There was no difference between hepatic MDA levels in rats fed with the SP diet and HFC diet at 4 W and also rats fed with SP diet and treated with HPE at 12 W.

Decreased hepatic glutathione levels indicate deterioration of antioxidant status in the liver. Hepatic GSH levels measured during the administration of the HFC diet and concurrent treatment with HPE in SHRSP5/Dmcr rats are presented in Figure 3B. The mean hepatic GSH levels were significantly decreased on 8 and 12 W compared with 4 W in the HFC diet group. Treatment with HPE resulted in restoration of normal levels of GSH on all the weeks studied. There was no difference between the mean GSH levels in rats fed with the SP diet and HFC diet at 4 W as well as rats fed with SP diet and treated with HPE at 12 W.

Clinical Science (2024) **138** 327–349
https://doi.org/10.1042/CS20230533

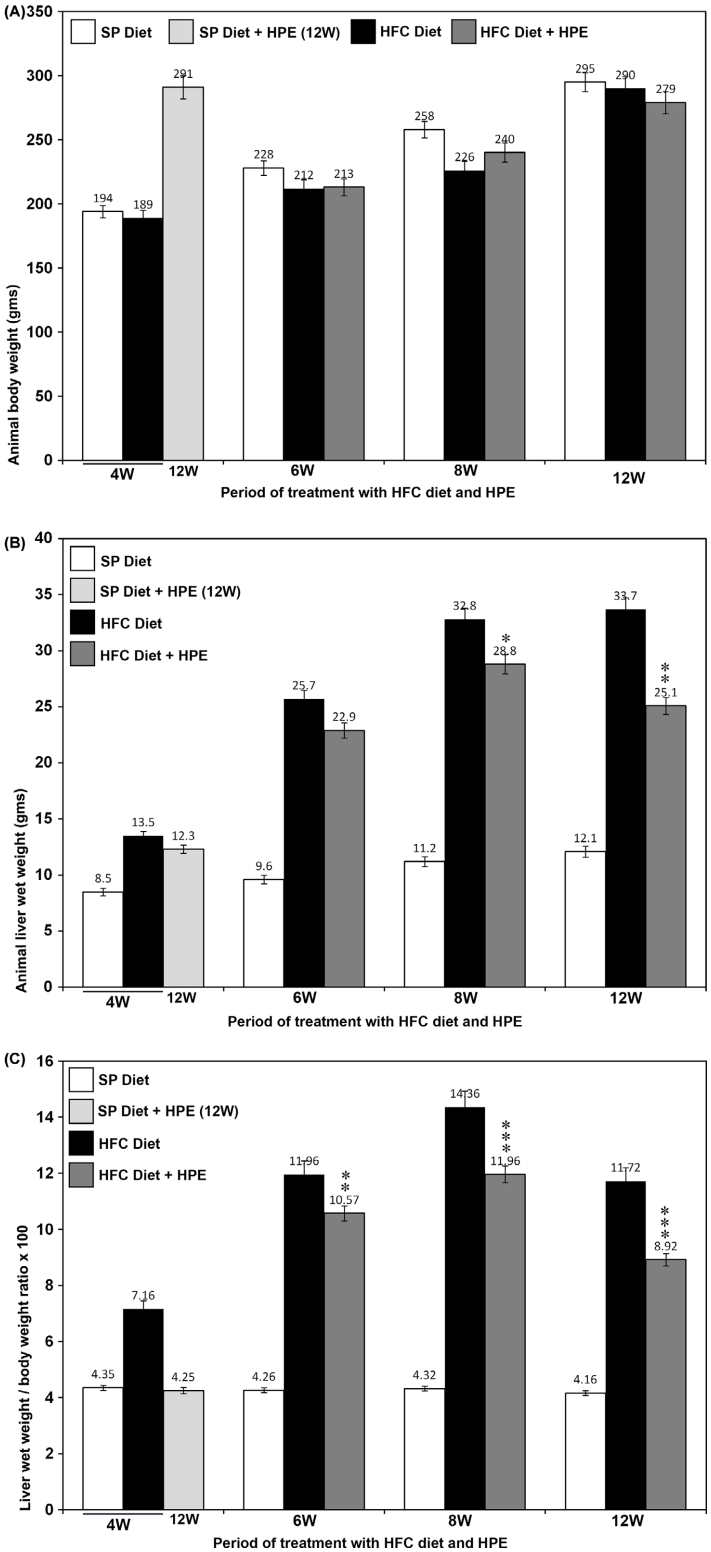

Figure 1. Body weight and liver wet weight as well as liver wet weight to body weight ratio of the animals treated with HFC diet and HPE

(**A**) Body weight. (**B**) Liver wet weight. There was significant reduction in liver wet weight at 8 and 12 W in HPE treated animals in the HFC diet group. (**C**) Liver wet weight to body weight ratio (×100). The liver weight to body weight ratio was significantly decreased at 6, 8, and 12 W in HPE treated animals of HFC diet group. $^{*}P<0.05$, $^{**}P<0.01$, and $^{***}P<0.001$ compared with the respective HFC diet controls by Student's *t*-test.

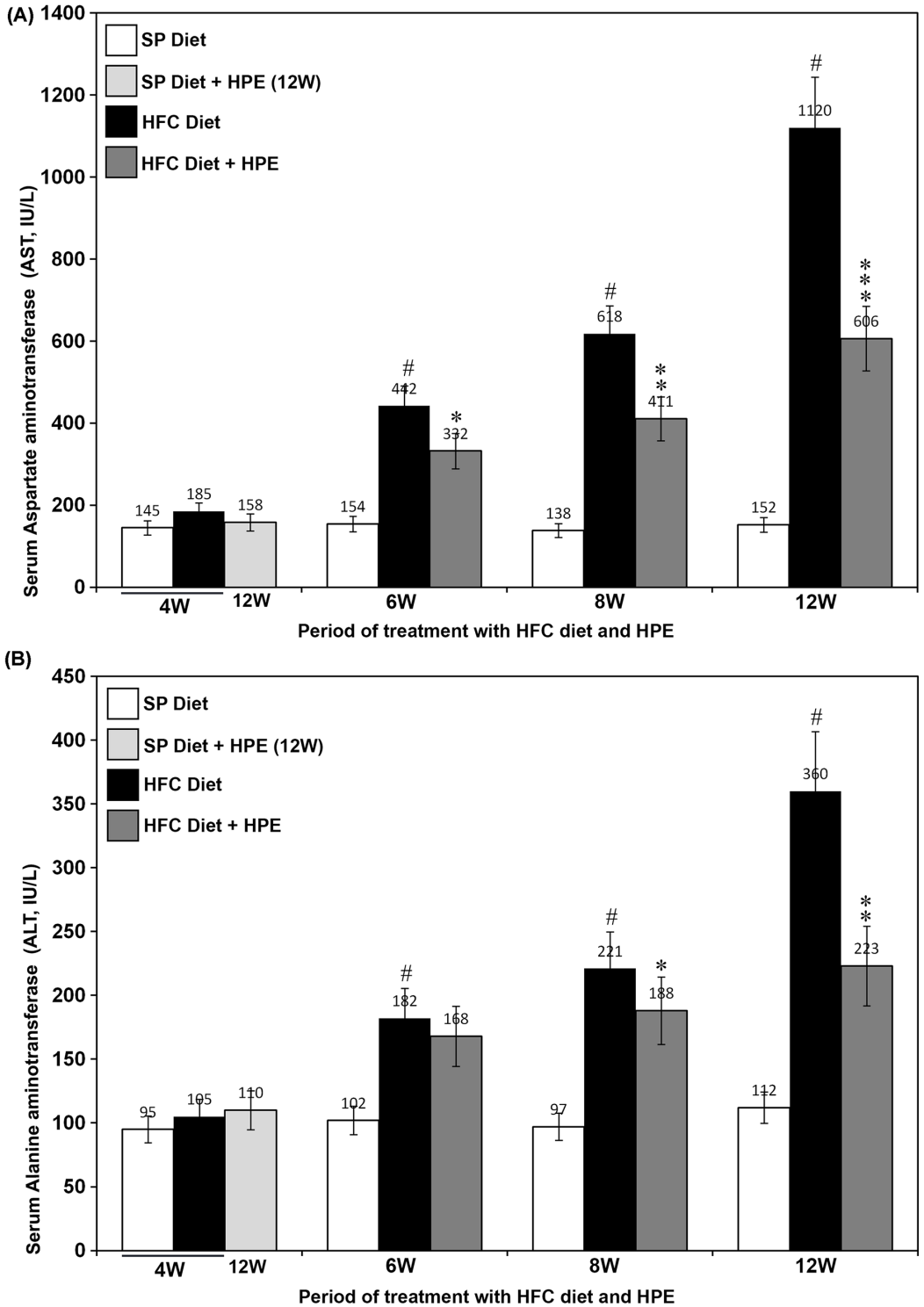

Figure 2. (A) Aspartate aminotransferase (AST) and (B) alanine aminotransferase (ALT) levels in the serum of SHRSP5/Dmcr rats fed with HFC diet for 12 weeks and after the treatment with HPE

Both AST and ALT levels were significantly increased at 6, 8, and 12 W compared with 4 W ($^{\#}P<0.001$ by ANOVA) in the HFC diet group. Treatment with HPE resulted in significant reduction of elevated AST and ALT levels in all the weeks studied except at 6th week in the case of ALT. There was no difference in the levels of AST and ALT between the rats fed with SP diet and HFC diet at 4 W. Similarly there was no difference in the levels of AST and ALT between the rats fed with SP diet and treated with HPE at 12 W. The data are mean $\pm$ S.D. of five rats in each group. $^{*}P<0.05$, $^{**}P<0.01$, and $^{***}P<0.001$ by Student's *t*-test compared with HFC diet group on respective weeks.

Clinical Science (2024) **138** 327–349
https://doi.org/10.1042/CS20230533

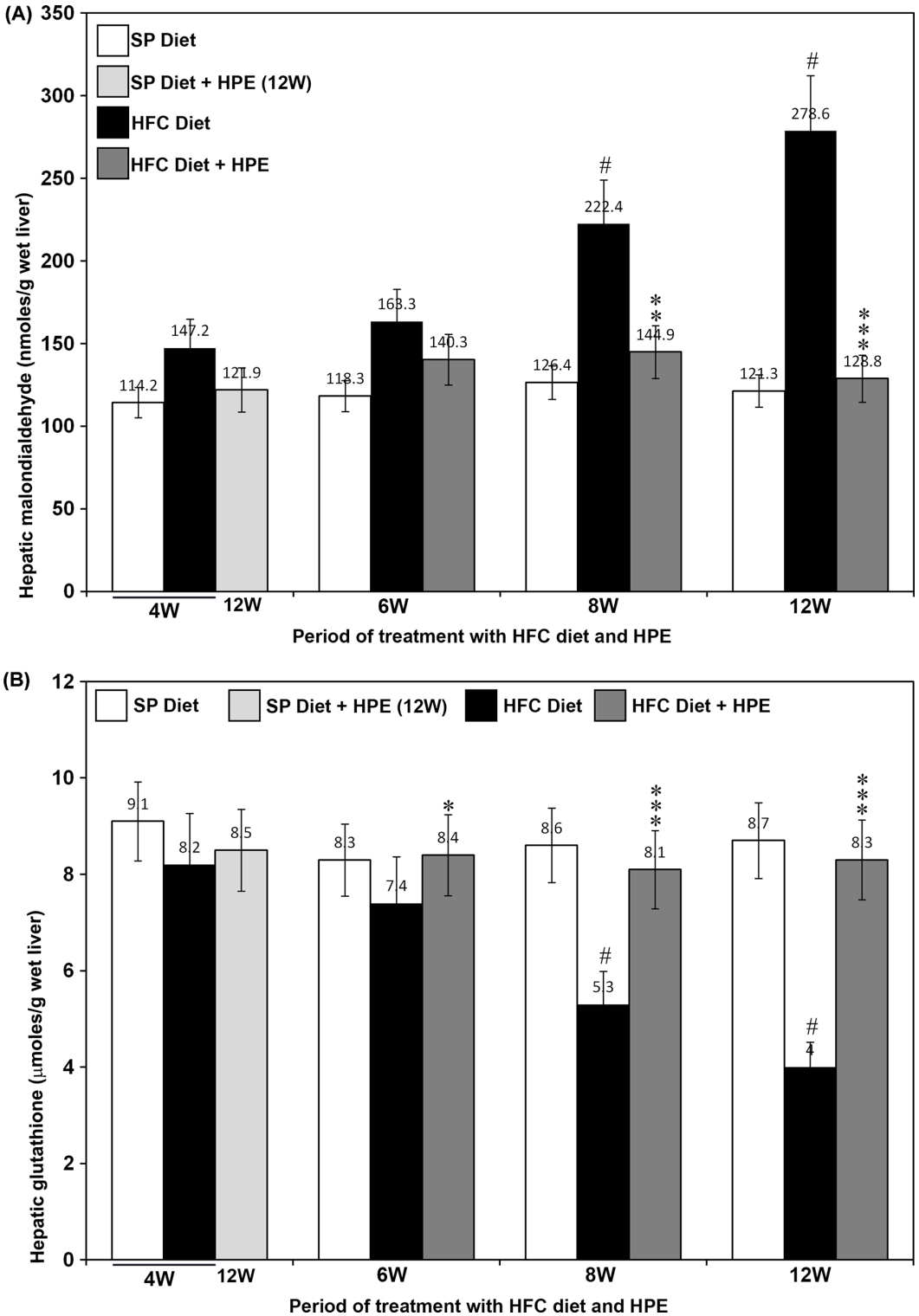

Figure 3. Hepatic malondialdehyde (MDA) and reduced glutathione (GSH) levels in SHRSP5/Dmcr rats fed with HFC diet for 12 weeks and after the treatment with HPE

(**A**) The hepatic MDA levels were markedly increased in the animals fed with HFC diet on 8 and 12 W compared with 4 W ($^{\#}P<0.001$ by ANOVA). Treatment with HPE resulted in restoration of normal levels of MDA on all the weeks studied. (**B**) Hepatic glutathione levels were significantly decreased on 8 and 12 W compared with 4 W in HFC diet group ($^{\#}P<0.001$ by ANOVA). Treatment with HPE resulted in restoration of normal levels of GSH on all the weeks evaluated. The data are mean ± S.D. of five rats in each group. $^{*}P<0.05$, $^{**}P<0.01$, and $^{***}P<0.001$ by Student's *t*-test compared with HFC diet group on respective weeks.

Histopathological evaluation of the pathogenesis of MASH and hepatic fibrosis and the effect of HPE treatment

The histopathological evaluation during the pathogenesis of HFC diet induced MASH and hepatic cirrhosis as well as the effect of HPE treatment in SHRSP5/Dmcr rats along with respective controls are presented in Figure 4. There were no histopathological alterations in the animals fed with SP diet at 4 weeks (Figure 4A). There was extensive deposition of fat globules in rats fed with HFC diet for 4 weeks. However, hepatic fibrosis or other histopathological alterations were not present (Figure 4B). There were no histopathological changes or deposition of fat globules in the livers of rats fed with SP diet and treated with HPE for 12 weeks (Figure 4C). There were no histopathological changes in the animals fed with SP diet for 6 weeks (Figure 4D). In the animals fed with HFC diet for 6 weeks, extreme fatty degeneration, mild hepatic inflammation, ballooning of hepatocytes, and periportal fibrosis were present indicating MASH (Figure 4E). In contrast, only fatty degeneration was present in the animals administered with HPE. Hepatic necrosis and inflammation were absent (Figure 4F). Histopathological alterations were absent in the animals fed with SP diet for 8 weeks (Figure 4G). At the 8th week of HFC diet, moderate hepatic necrosis, sinusoidal congestion, incomplete nodule formation, and vacuolization of hepatocytes were present. Bridging fibrosis and deposition of collagen fibers were prominent (Figure 4H). However, only moderate steatosis of hepatocytes and slight necrosis were present in the livers of rats treated with HPE. Bridging fibrosis and deposition of collagen fibers were absent (Figure 4I). Significant pathological alterations were absent in the livers of rats fed with SP diet for 12 weeks (Figure 4J). Well developed fibrosis and early cirrhosis with nodule formation were present in rats fed with HFC diet for 12 weeks (Figure 4K). Extensive deposition of thick, mature collagen fibers was prominent (Figure 4K). At 12 weeks, treatment with HPE markedly reduced hepatic fibrosis and the deposition of collagen fibers in the hepatic parenchyma. Besides, hepatic inflammation and ballooning of hepatocytes were significantly decreased (Figure 4L). There was progressive bridging, but nodule formation was absent. Moderate pericentral fibrosis was present (Figure 4L). The SAF score is presented as 0–3 grades below the representative image from each group in Figure 4.

Treatment with HPE prevented deposition of collagen in the liver

Azan trichrome staining for collagen in SHRSP5/Dmcr rats fed with HFC diet and after treatment with HPE is presented in Figure 5. Staining for collagen was absent in the hepatic parenchyma of rats fed with SP diet at 4 weeks (Figure 5A). Similarly, there was no staining for collagen deposition in the liver of animals fed with HFC diet for 4 weeks (Figure 5B). There was no newly formed collagen in the hepatic tissue of rats fed with SP diet and treated with HPE for 12 weeks (Figure 5C). The staining for collagen depicted normal liver in the animals fed with SP diet for 6 weeks (Figure 5D). At 6th week of HFC diet, there was moderate staining of thin collagen fibers in the hepatic parenchyma and initiation of bridging fibrosis (Figure 5E). However, only slight periportal staining for collagen was present in the animals administered with HPE (Figure 5F). Staining for newly formed collagen was absent in the liver tissue of animals fed with SP diet for 8 weeks (Figure 5G). Marked staining depicting deposition of thick collagen fibers with well developed bridging fibrosis was present in the hepatic parenchyma of rats fed with HFC diet for 8 weeks (Figure 5H). There was prominent pericentral fibrosis with the formation of fibrous septa (Figure 5H). Treatment with HPE resulted in a significant decrease in staining for collagen, prevented bridging fibrosis, and formation of fibrous septa (Figure 5I). There was no staining for collagen in the hepatic parenchyma of rats fed with SP diet for 12 weeks (Figure 5J). In rats fed with HFC diet for 12 weeks, there was remarkable and intense staining of thick collagen fibers with nodule formation demonstrating severe hepatic fibrosis and cirrhosis (Figure 5K). In contrast, the HPE administered rats depicted only focal fibrosis with incomplete fibrous septa and partial bridging (Figure 5L). There was marked reduction in collagen staining and deposition of newly synthesized collagen fibers (Figure 5L).

Treatment with HPE inhibited activation of hepatic stellate cells

Activation and transformation of quiescent hepatic stellate cells into myofibroblast like cells with the expression of α-SMA marks the first step in the pathogenesis of hepatic fibrosis [31]. The results of the immunohistochemical staining for the expression of α-SMA in paraffin liver sections of SHRSP5/Dmcr rats fed with HFC diet and after the administration of HPE are demonstrated in Figure 6. Staining for α-SMA was completely absent in the hepatic parenchyma of SHRSP5/Dmcr rats fed with HFC diet for 4 weeks (Figure 6A). There was no staining for α-SMA in the hepatic parenchyma of rats fed with SP diet and treated with HPE for 12 weeks (Figure 6B). There was prominent staining for α-SMA in the fibrotic zones, especially in the areas with bridging fibrosis in the animals fed with HFC diet for 6 weeks (Figure 6C). In contrast, there was no staining for α-SMA in the hepatic parenchyma of rat livers administered with HFC diet and HPE (Figure 6D). At the 8th week, HFC fed rat livers depicted obvious and marked staining for α-SMA indicating activation of enormous hepatic stellate cells, especially in fibrotic zones (Figure 6E).

Clinical Science (2024) **138** 327–349
https://doi.org/10.1042/CS20230533

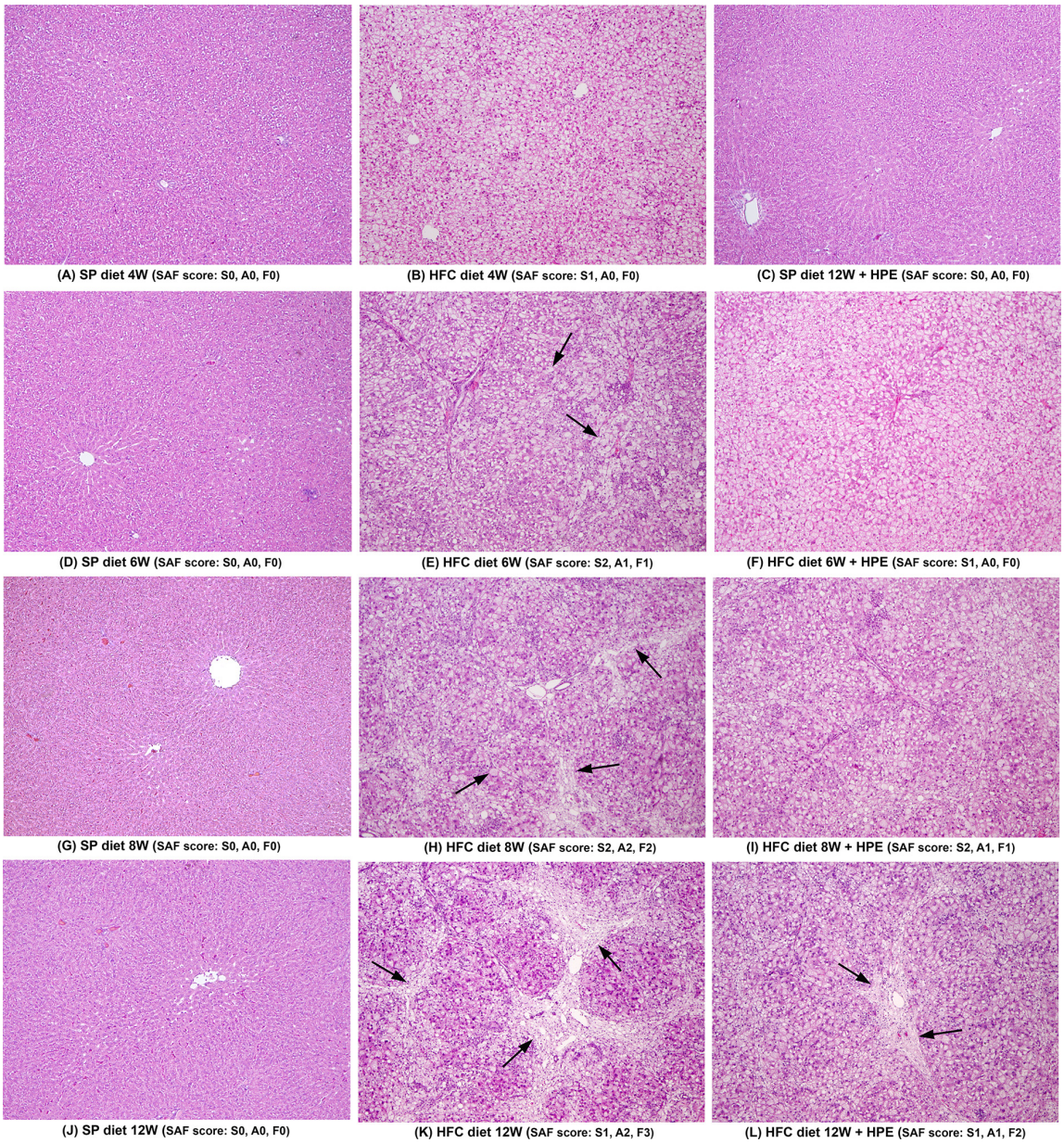

Figure 4. Hematoxylin and Eosin staining in SHRSP5/Dmcr rats fed with HFC diet for 12 weeks and after the treatment with HPE

(**A**) SP diet 4 W. Normal liver without any pathological alterations. (**B**) HFC diet 4 W. Presence of simple steatosis in the entire hepatic parenchyma indicating deposition of fat globules. Liver fibrosis and inflammation was completely absent. (**C**) SP diet 12 W with HPE treatment. Significant pathological alteration was absent after 12 weeks of SP diet and HPE treatment. (**D**) SP diet 6 W. Pathological alterations were absent. (**E**) HFC diet 6 W. Fatty degeneration, mild hepatic inflammation, and ballooning of hepatocytes were present especially in the periportal areas (arrows). Mild periportal fibrosis was also observed. (**F**) HFC diet 12 W with HPE treatment 6 W. Fatty degeneration was present in the hepatic parenchyma. Hepatic necrosis and inflammation were absent. (**G**) SP diet 8 W. There were no pathological alterations. (**H**) HFC diet 8 W. Hepatic necrosis, sinusoidal congestion, and vacuolization of hepatocytes were present. Bridging fibrosis and formation of collagen fibers were prominent (arrows). (**I**) HFC diet 8 W with HPE treatment. Mild steatosis of hepatocytes and slight necrosis were present. Bridging fibrosis was absent. (**J**) SP diet 12 W. Significant pathological alterations were absent. (**K**) HFC diet 12 W. There was well developed fibrosis and early cirrhosis with deposition of mature collagen fibers (arrows). (**L**) HFC diet 12 W with HPE treatment. Treatment with HPE significantly reduced liver fibrosis and deposition of collagen fibers in the hepatic parenchyma. Hepatic inflammation and ballooning of hepatocytes were markedly reduced. Moderate pericentral fibrosis was present (arrow). All images are original magnification, ×40. The SAF score, steatosis (S0-3), activity (A0-3), and fibrosis (F0-3) are presented below each representative image.

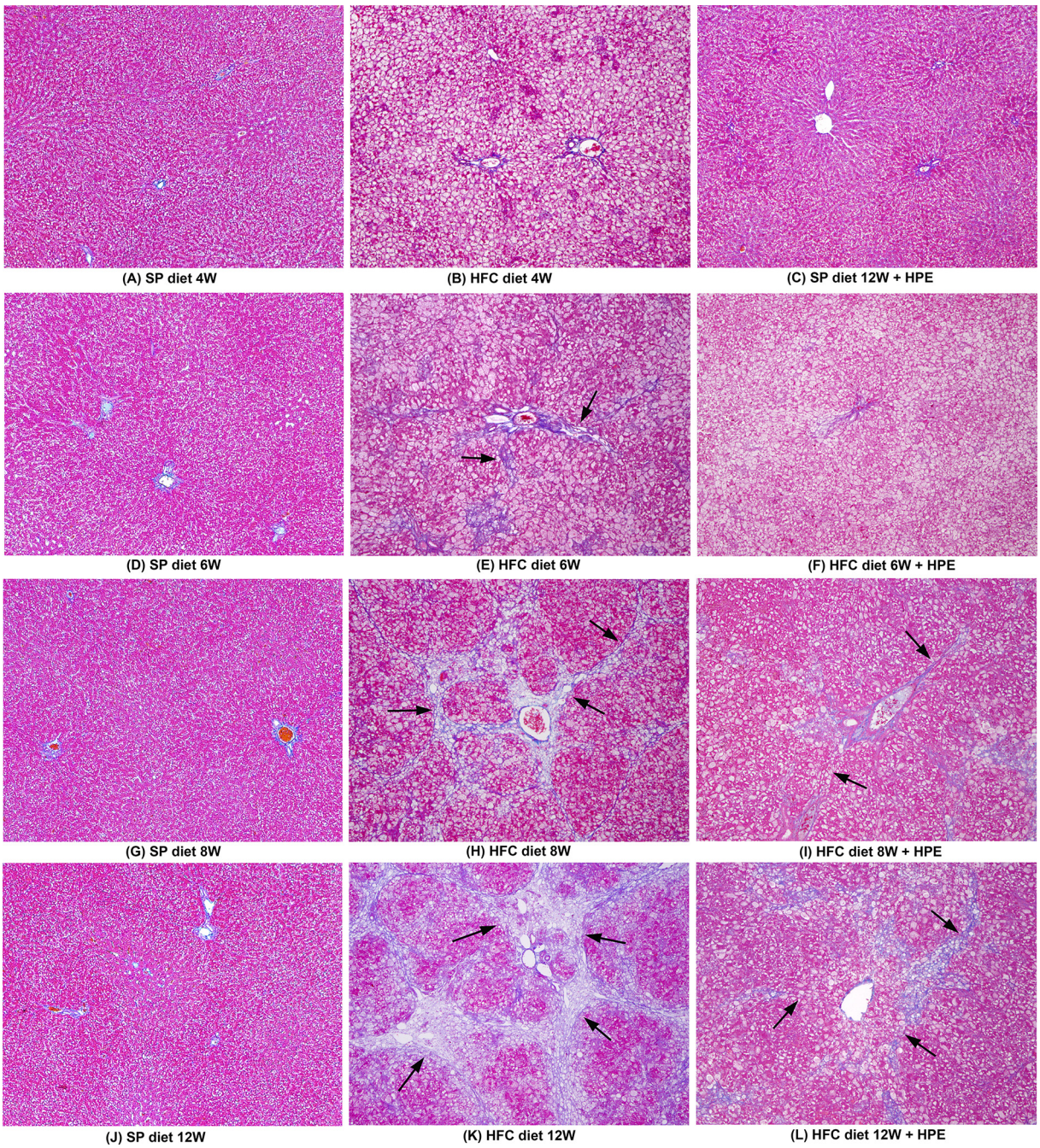

Figure 5. Azan trichrome staining for collagen in SHRSP5/Dmcr rats fed with HFC diet for 12 weeks and after the treatment with HPE

(**A**) SP diet 4 W. Staining for collagen was absent in the hepatic parenchyma. (**B**) HFC diet 4 W. Absence of collagen staining. (**C**) SP diet 12 W with HPE treatment. Staining for collagen was absent. (**D**) SP diet 6 W. No staining for collagen. (**E**) HFC diet 6 W. Moderate staining of collagen fibers and initiation of bridging fibrosis (arrows). (**F**) HFC diet 6 W with HPE treatment. Slight staining for collagen in the periportal area. (**G**) SP diet 8 W. There was no staining for collagen. (**H**) HFC diet 8 W. Prominent staining for collagen depicting formation of thick collagen fibers with well developed bridging fibrosis in the hepatic parenchyma (arrows). (**I**) HFC diet 8 W with HPE treatment. Significant decrease in staining for collagen and absence of bridging fibrosis (arrows). (**J**) SP diet 12 W. There was no staining for collagen in the hepatic parenchyma. (**K**) HFC diet 12 W. Marked and intense staining of collagen fibers depicting well developed bridging fibrosis and early cirrhosis (arrows). (**L**) HFC diet 12 W with HPE treatment. Conspicuous reduction in collagen staining compared with the animals without HPE treatment. Focalized fibrosis with incomplete fibrous septa and partial bridging were present (arrows). All images are original magnification, ×40.

Clinical Science (2024) **138** 327–349
https://doi.org/10.1042/CS20230533

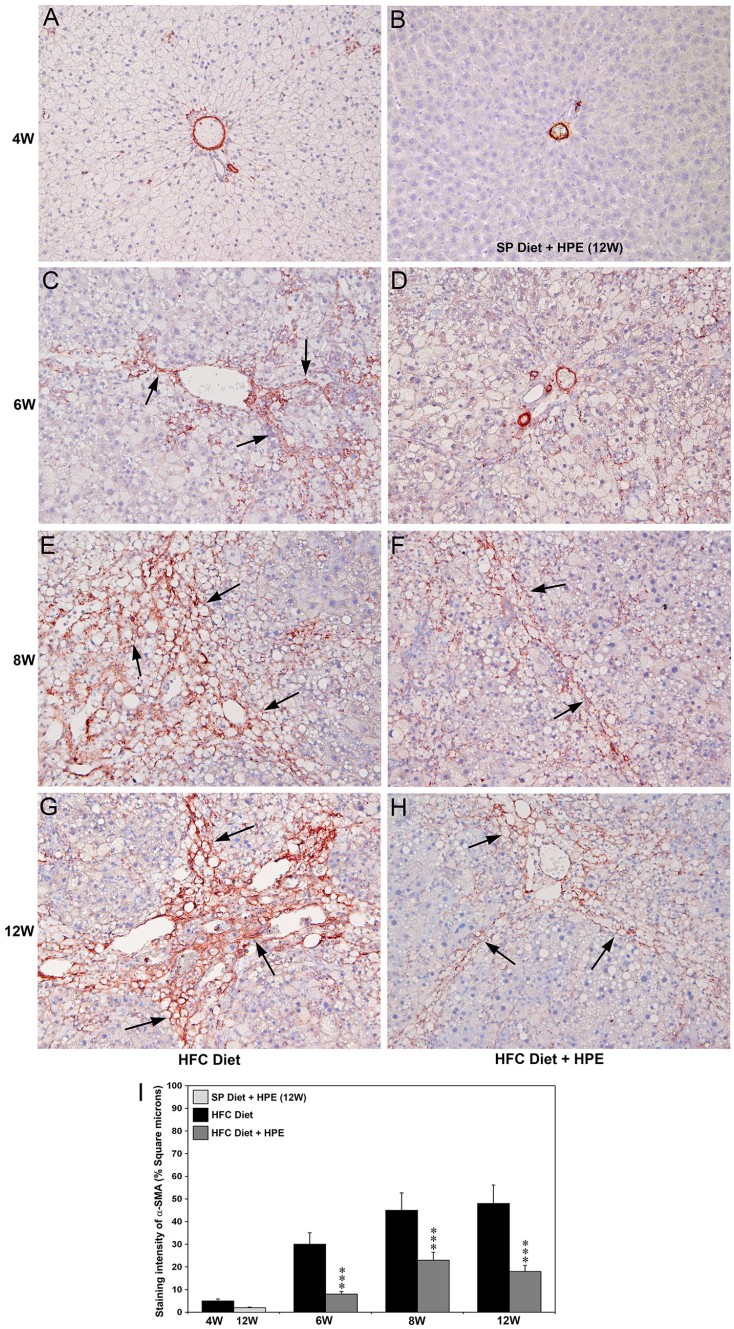

Figure 6. Immunohistochemical staining for α-SMA in SHRSP5/Dmcr rats fed with HFC diet for 12 weeks and after the treatment with HPE

(**A**) HFC diet 4 W. Staining for α-SMA was absent in the hepatic parenchyma. (**B**) SP diet 12 W with HPE treatment. There was no staining for α-SMA in the hepatic parenchyma. (**C**) HFC diet 6 W. Prominent staining for α-SMA in the fibrotic zones, especially in the areas with initiation of bridging fibrosis (arrows). (**D**) HFC diet 6 W with HPE treatment. There was no staining for α-SMA in the hepatic parenchyma of rat livers treated with HPE. (**E**) HFC diet 8 W. Enormous and obvious staining for α-SMA in the hepatic parenchyma with fibrosis (arrows). (**F**) HFC diet 8 W with HPE treatment. The staining for α-SMA was remarkably reduced in rats treated with HPE (arrows). (**G**) HFC diet 12 W. Strong and marked staining for α-SMA in the fibrotic areas indicating extensive activation of hepatic stellate cells (arrows). (**H**) HFC diet 12 W with HPE treatment. Significant reduction of staining for α-SMA in the hepatic parenchyma and also in areas with fibrosis (arrows). All images are original magnification, ×100. (I) Quantification of the staining intensity of α-SMA. The intensity of α-SMA staining was quantified using Image-Pro Discovery software and presented as percent square microns. The data are mean ± S.D. of 10 randomly selected microscopic fields from five rats per group. ***$P<0.001$ by Student's *t*-test compared with the HFC diet group on respective weeks.

The staining for α-SMA was remarkably reduced in rats treated with HPE and was restricted only to the areas with thin collagen fibers (Figure 6F). At 12th week of HFC diet, there was strong and marked staining for α-SMA in the fibrotic areas, indicating extensive activation of hepatic stellate cells (Figure 6G). Treatment with HPE demonstrated a significant reduction of α-SMA staining in the hepatic parenchyma and also in areas with fibrosis (Figure 6H). Quantification of the staining intensity of α-SMA presented as square microns demonstrated significant reduction ($P<0.001$) after treatment with HPE on all the weeks studied (Figure 6I).

Administration of HPE remarkably reduced oxidative stress

Increased production of 4-hydroxy-2-nonenal (4-HNE) is considered as a potent marker of reactive oxygen species (ROS) induced lipid peroxidation of polyunsaturated fatty acids and dramatically increases during pathogenesis of MASH [32]. The results of the immunohistochemical staining of 4-HNE in paraffin liver sections of SHRSP5/Dmcr rats fed with HFC diet and after the administration of HPE are demonstrated in Figure 7. Staining for 4-HNE was completely absent in the liver tissue of SHRSP5/Dmcr rats fed with HFC diet for 4 weeks (Figure 7A). Similarly, staining for 4-HNE was absent in the livers of rats fed with the SP diet and treated with HPE for 12 weeks (Figure 7B). There was moderate staining of 4-HNE, especially in the pericentral areas of the animals fed with HFC diet for 6 weeks (Figure 7C). However, there was only slight staining of 4-HNE in the pericentral areas of rat livers treated with HPE (Figure 7D). At the 8th week, there was prominent and obvious staining for 4-HNE in the entire hepatic parenchyma (Figure 7E). The staining was remarkably reduced in rats treated with HPE and only mild staining was present in the pericentral area (Figure 7F). At the 12th week of HFC diet, there was marked and intense staining for 4-HNE in the entire hepatic parenchyma, especially areas close to fibrosis zone (Figure 7G). In contrast, HPE treated rat livers depicted marked reduction of 4-HNE staining in the hepatic parenchyma (Figure 7H). Only moderate staining was present in the pericentral areas (Figure 7H). Measurement of the staining intensity of 4-HNE presented as percentage square microns depicted significant reduction ($P<0.001$) after treatment with HPE on all the weeks evaluated (Figure 7I).

Treatment with HPE prevented accumulation of collagen type I in the hepatic parenchyma

The accumulation of fibril forming collagens in the extracellular matrix of the liver is the most prominent characteristic feature during the pathogenesis of hepatic fibrosis [33]. The results of the immunohistochemical staining of collagen type I in the liver sections of SHRSP5/Dmcr rats fed with HFC diet and after treatment with HPE are depicted in Figure 8. Staining for collagen type I was absent or very feeble in the hepatic parenchyma of SHRSP5/Dmcr rats fed with HFC diet for 4 weeks (Figure 8A). There was no staining for collagen type I in the hepatic parenchyma of rats fed with the SP diet and treated with HPE for 12 weeks (Figure 8B). At 6 W of HFC diet, moderate staining for collagen type I was present in the fibrotic areas (Figure 8C). However, only mild staining was present in rats administered with HPE (Figure 8D). At the 8th week of HFC diet, marked and conspicuous staining for collagen type I was present in the fibrotic zone with deposition of mature collagen fibers (Figure 8E). Treatment with HPE resulted in a marked reduction of collagen type I staining and was restricted to the areas with bridging fibrosis (Figure 8F). At the 12th week of HFC diet, there was intense and remarkable staining for collagen type I in the fibrotic areas indicating deposition of enormous amount of newly formed collagen (Figure 8G). In rats administered with HPE, staining for collagen type I was completely absent in the hepatic parenchyma (Figure 8H). Weak staining was present on thin collagen fibers with incomplete fibrous septa (Figure 8H). Quantification of the staining intensity of collagen type I presented as square microns demonstrated remarkable reduction ($P<0.001$) after treatment with HPE on all the weeks studied (Figure 8I).

Administration of HPE inhibited early deposition of collagen type III during pathogenesis of MASH

The results of the immunohistochemical staining of collagen type III in the paraffin liver sections of SHRSP5/Dmcr rats fed with HFC diet and after the administration of HPE are demonstrated in Figure 9. At 4 W of HFC diet, focalized staining for collagen type III was present in areas with early bridging fibrosis (Figure 9A). Staining for collagen type III was completely absent in the livers of rats fed with SP diet and administered HPE for 12 weeks (Figure 9B). At 6 W of HFC diet, significant staining for collagen type III was present as chicken wire pattern in the fibrotic zone (Figure 9C). However, in rats treated with HPE, only mild staining was present in the bridging areas (Figure 9D). At the 8th week of HFC diet, marked and prominent staining for collagen type III was present in fibrotic areas with well developed collagen fibers (Figure 9E). In rats administered with HPE, staining for collagen type III was significantly

Clinical Science (2024) **138** 327–349
https://doi.org/10.1042/CS20230533

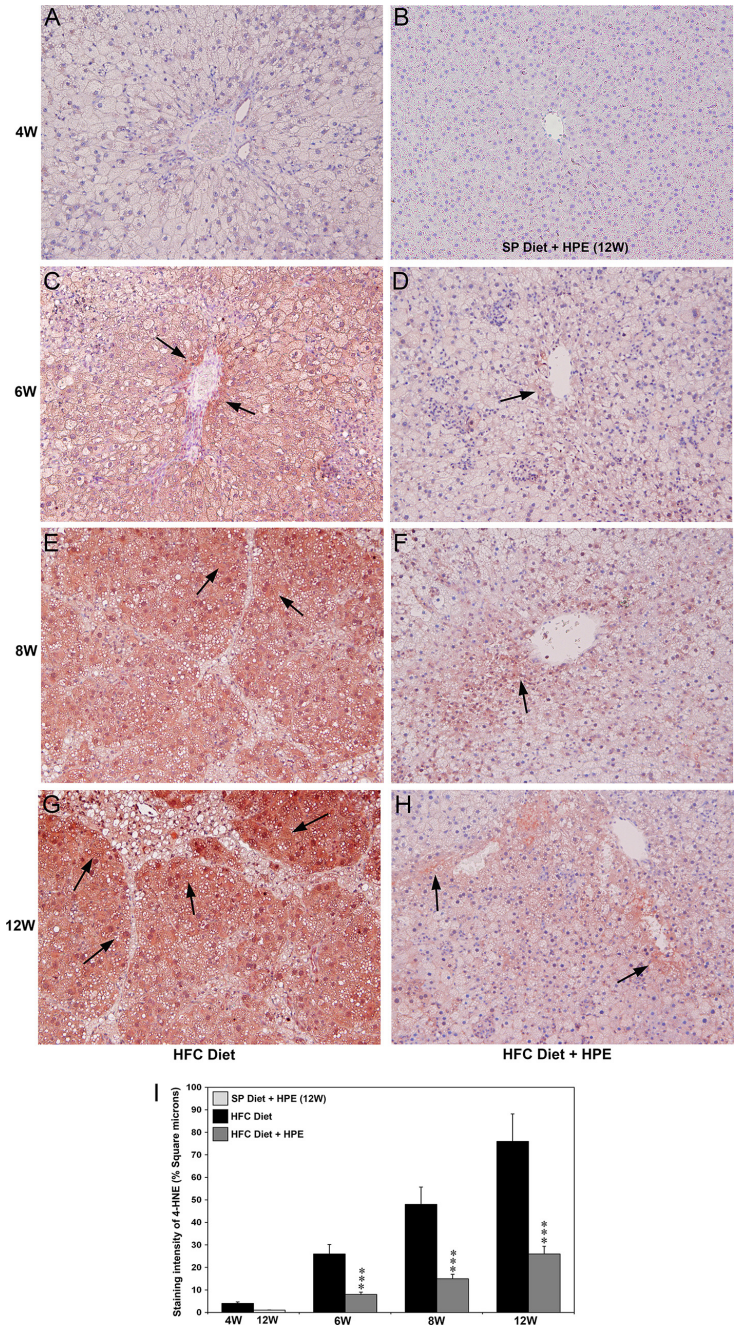

Figure 7. Immunohistochemical staining for 4-hydroxy-2-nonenal (4-HNE) in SHRSP5/Dmcr rats fed with HFC diet for 12 weeks and after the treatment with HPE

(**A**) HFC diet 4 W. Staining for 4-HNE was completely absent in the hepatic parenchyma. (**B**) SP diet 12 W with HPE treatment. Absence of 4-HNE staining. (**C**) HFC diet 6 W. At 6 W of HFC diet, there was moderate staining of 4-HNE in the pericentral areas (arrows). (**D**) HFC diet 6 W with HPE treatment. Slight staining for 4-HNE in the pericentral areas of rat livers treated with HPE (arrow). (**E**) HFC diet 8 W. Prominent and obvious staining for 4-HNE was present in the entire hepatic parenchyma (arrows). (**F**) HFC diet 8 W with HPE treatment. The staining of 4-HNE was remarkably reduced in rats treated with HPE. Presence of mild staining in pericentral areas (arrow). (**G**) HFC diet 12 W. There was marked and strong staining of 4-HNE in the entire hepatic parenchyma, especially in areas close to fibrosis zone (arrows). (**H**) HFC diet 12 W with HPE treatment. HPE treated rat livers depicted remarkable reduction of 4-HNE staining in the hepatic parenchyma. Only moderate staining was present in the pericentral areas (arrows). All images are original magnification, $\times$100. (**I**) Quantification of the staining intensity of 4-HNE. The staining intensity of 4-HNE was quantified using Image-Pro Discovery software and presented as percent square microns. The data are mean $\pm$ S.D. of 10 randomly selected microscopic fields from five rats per group. ***$P<0.001$ by Student's *t*- test compared with the HFC diet group on respective weeks.

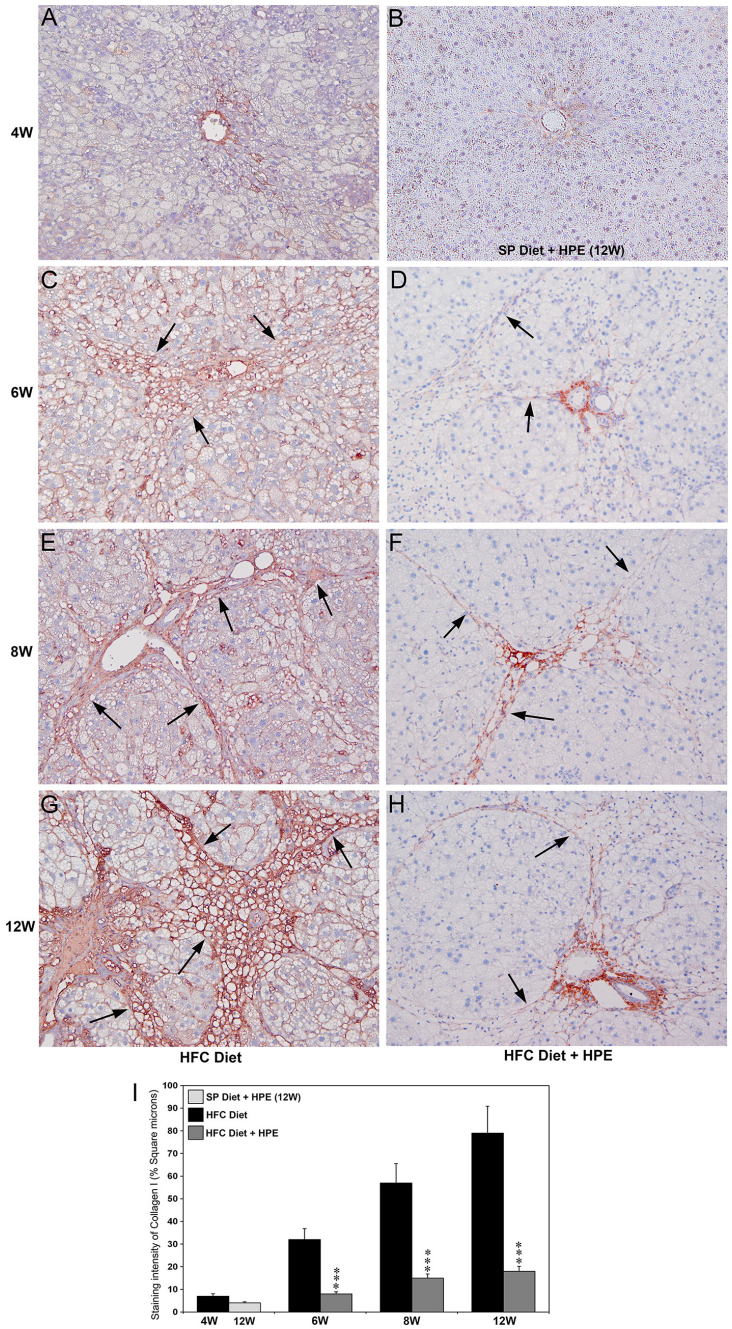

Figure 8. Immunohistochemical staining for collagen type I in SHRSP5/Dmcr rats fed with HFC diet for 12 weeks and after the treatment with HPE

(**A**) HFC diet 4 W. Staining for collagen type I was absent or very feeble in the hepatic parenchyma. (**B**) SP diet 12 W with HPE treatment. Staining for collagen type I was absent in the parenchyma. (**C**) HFC diet 6 W. At 6 W of HFC diet, moderate staining for collagen type I was present in the fibrotic areas (arrows). (**D**) HFC diet 6 W with HPE treatment. Weak staining on thin collagen fibers (arrows). (**E**) HFC diet 8 W. Marked and conspicuous staining for collagen type I was present in the fibrotic zone with mature collagen fibers (arrows). (**F**) HFC diet 8 W with HPE treatment. The staining for collagen type I was obviously reduced in rats treated with HPE and was confined to thin collagen fibers (arrows). (**G**) HFC diet 12 W. Strong and remarkable staining for collagen type I in the fibrotic areas indicating deposition of enormous amount of newly formed collagen (arrows). (**H**) HFC diet 12 W with HPE treatment. In the rats treated with HPE, staining for collagen type I was completely absent in the hepatic parenchyma. Weak staining was present on thin collagen fibers with incomplete fibrous septa (arrows). All images are original magnification, $\times$100. (**I**) Quantification of the staining intensity of collagen type I presented as percent square microns. The data are mean $\pm$ S.D. of 10 randomly selected microscopic fields from five rats per group. ***$P<0.001$ by Student's *t*-test compared with the HFC diet group on respective weeks.

Clinical Science (2024) **138** 327–349
https://doi.org/10.1042/CS20230533

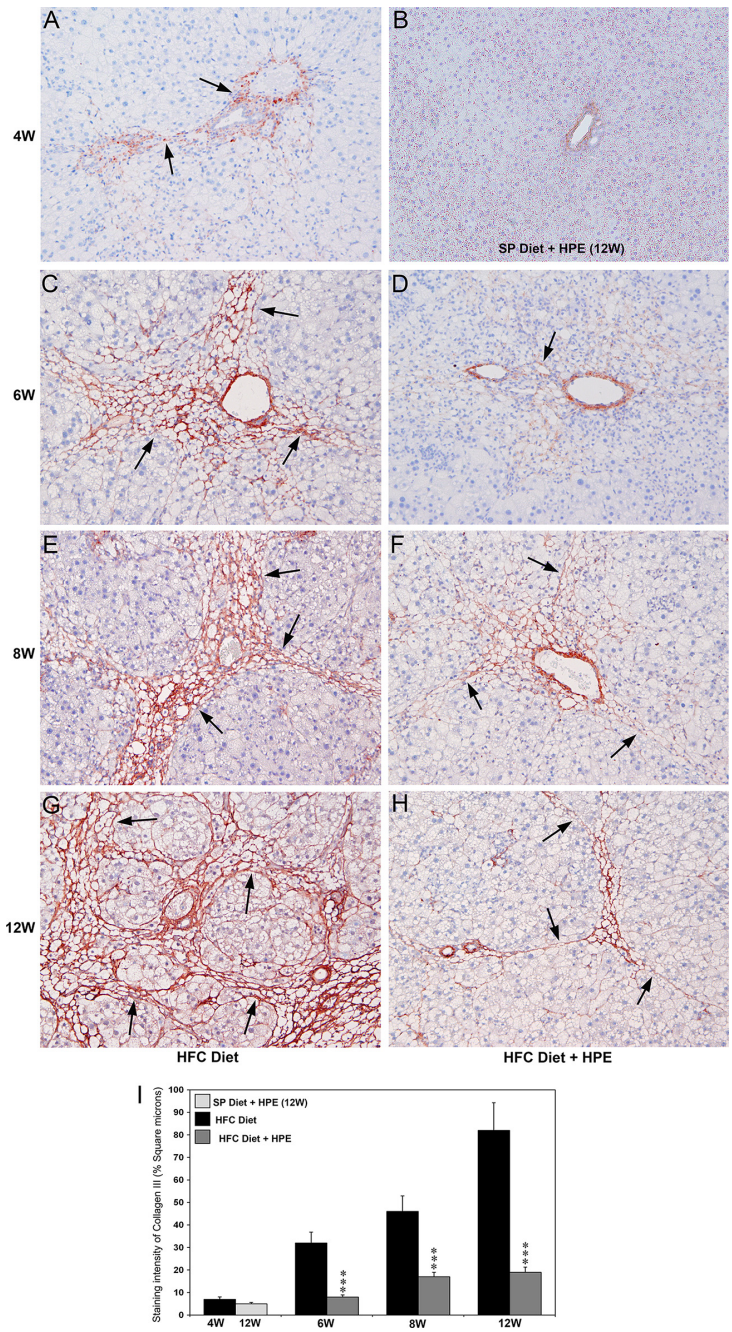

Figure 9. Immunohistochemical staining for collagen type III in SHRSP5/Dmcr rats fed with HFC diet for 12 weeks and after the treatment with HPE

(**A**) HFC diet 4 W. Weak staining for collagen type III was present in the areas with initiation of bridging (arrows). (**B**) SP diet 12 W with HPE treatment. Staining for collagen type III was absent in the hepatic parenchyma. (**C**) HFC diet 6 W. At 6 W of HFC diet, significant staining was present for collagen type III in the fibrotic zone (arrows). (**D**) HFC diet 6 W with HPE treatment. Mild staining for collagen was present in the areas with bridging fibrosis (arrow). (**E**) HFC diet 8 W. Marked and prominent staining for collagen type III was present in fibrotic areas with well developed collagen fibers (arrows). (**F**) HFC diet 8 W with HPE treatment. Staining for collagen type III was significantly decreased and was restricted to thin collagen fibers (arrows). (**G**) HFC diet 12 W. Remarkable and profound staining for collagen type III demonstrating deposition of newly synthesized collagen (arrows). (**H**) HFC diet 12 W with HPE treatment. Staining for collagen type III was completely absent in the hepatic parenchyma of rat livers treated with HPE. Moderate staining was visible on thin collagen fibers present (arrows). All images are original magnification, $\times$100. (**I**) Quantification of the staining intensity of collagen type III presented as percent square microns. The data are mean $\pm$ S.D. of 10 randomly selected microscopic fields from five rats per group. ***$P<0.001$ by Student's *t*-test compared with the HFC diet group on respective weeks.

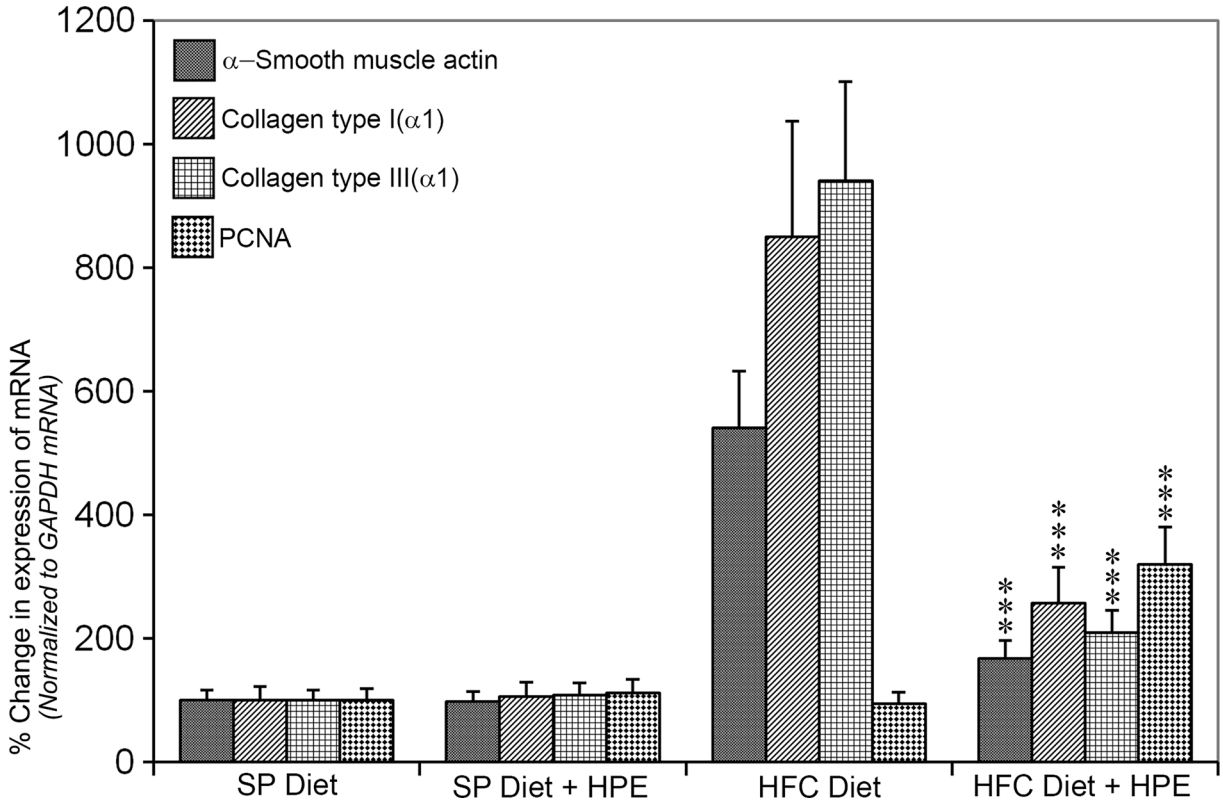

Figure 10. Real-time quantitative PCR for the expression of α-SMA, collagen type I(α1), collagen type III(α1), and PCNA in SHRSP5/Dmcr rats fed with HFC diet for 12 weeks and after the treatment with HPE

There was marked increase in the expression of all the molecules studied after the administration of HFC diet for 12 weeks, which were significantly decreased in HPE treated group. All the data are normalized to GAPDH mRNA that serves as the housekeeping gene. The data are mean ± S.D. of five rats in each group. ***$P<0.001$ by ANOVA, when compared with the respective HFC diet group.

decreased and was confined to the chicken wire pattern of collagen fibers (Figure 9F). At 12th week of HFC diet, remarkable and profound staining of collagen type III was present depicting well developed nodular cirrhosis (Figure 9G). Furthermore, the staining demonstrated deposition of large amount of newly synthesized collagen type III in the hepatic parenchyma (Figure 9G). In contrast, staining for collagen type III was completely absent in the hepatic parenchyma of rat livers treated with HPE (Figure 9H). Moderate staining was visible on thin collagen fibers (Figure 9H). Quantification of the staining intensity of collagen type III presented as percentage square microns depicted a marked reduction ($P<0.001$) after treatment with HPE on all the weeks evaluated (Figure 9I).

Treatment with HPE decreased the expression of major molecules involved in hepatic fibrosis

The isolated mRNA was quantified for the expression of α-SMA, collagen type I(α1), and collagen type III(α1) in the liver tissue to study the effect of HPE to attenuate fibrogenesis and PCNA as a cell proliferative marker that indicates the regeneration of liver tissue. The rate of expression of mRNA of all the molecules examined was normalized to the GAPDH gene and presented in Figure 10. There was no difference in the expression of any of the molecules studied between the SP diet group and SP diet group treated with HPE. Dramatic increase in the expression of all the fibrogenic markers studied was present in the HFC diet group of animals. The maximum increase (9.4-fold) was observed with collagen type III, followed by collagen type I (8.5-fold) compared with the SP diet group. The increased molecular markers were remarkably decreased ($P<0.001$ by ANOVA) in the HPE-treated group. There was no difference in the expression of PCNA in the HFC diet group, which was significantly increased ($P<0.001$ by ANOVA) after the treatment with HPE.

Clinical Science (2024) **138** 327–349
https://doi.org/10.1042/CS20230533

Discussion

Simple steatosis is a condition of increased uptake and deposition of lipids or fat in hepatocytes. Unmanaged simple steatosis may progress to metabolic dysfunction-associated steatohepatitis (MASH) with inflammation, hepatocellular injury, fibrosis, cirrhosis, and ultimate HCC [34]. In the present study, we used a high-fat and high-cholesterol diet induced animal model of steatohepatitis, which spontaneously progresses to hepatic fibrosis and cirrhosis [24]. It is a model similar to human MASH with all the associated biochemical, histopathological, and decompensating features [24]. In addition, it provides a reproducible and potentially valuable animal model for studying the mechanism of the pathogenesis of human hepatic fibrosis and alcoholic cirrhosis without employing a chemical agent such as carbon tetrachloride or N-nitrosodimethylamine [28,35]. Overall, the HFC-induced model of MASH, hepatic fibrosis, and liver cirrhosis in SHRSP5/Dmcr rats is an ideal and suitable animal model to study multiple parameters of human pathological conditions in a natural way.

Laennec is the trade name for human placental extract, which has been selectively prepared after acid hydrolysis and enzymatic digestion. It is manufactured after treatment with dilute hydrochloric acid and pepsin digestion, followed by high-pressure steam sterilization at 121°C for 20 min, and tested for all human pathogenic viral DNAs and RNAs [36]. These processes ensure that Laennec is free from all sorts of transmissible human pathogens such as HIV, HBV, HCV, HPV, HSV as well as bacteria and funguses. The product used in the present study contains a variety of growth factors, cytokines, and physiologically active substances from the human placenta [37]. It contains hepatocyte growth factor (HGF), which promotes proliferation of hepatocytes for the recovery and regeneration of injured or damaged liver. Recently, a pilot study demonstrated that administration of HPE for 8 weeks in patients with MASH resulted in a significant reduction of serum AST and ALT levels, indicating HPE could be used as an effective method to treat MASH [38]. It was also shown that HPE treatment suppresses activation of hepatic stellate cells and ameliorates hepatic fibrosis in methionine and choline deficient (MCD) diet-induced model of MASH [36]. Furthermore, it has been demonstrated that HPE treatment decreases inflammation, reduces fibrosis, and promotes liver regeneration, suggesting the use of HPE for potential clinical applications [37].

During the pathogenesis of hepatic fibrosis, defenestration of endothelial cells leads to increased diffusion barrier and interferes with the transport of nutrients to hepatocytes, which contributes to the deterioration of liver functions [39]. It was reported that HPE treatment significantly reduced serum AST and ALT levels along with up-regulation of anti-inflammatory cytokines and promoted liver regeneration in CCl_4 induced liver injury in rats [37]. Furthermore, HPE administration decreased serum AST and ALT levels and reduced lobular inflammation and hepatocyte ballooning in obese patients with MASH [38]. In the present study, we observed a significant decrease in both AST and ALT levels in the serum of rats treated with HPE for 8 and 12 W. This could be attributed to the anti-inflammatory, antioxidant, and hepatocyte regeneration factors present in HPE [40]. In the current study, treatment with HPE decreased hepatic inflammation, sinusoidal congestion, hepatic necrosis, and vacuolization of hepatocytes in rats fed with HFC diet. Besides, HPE treatment reduced fatty degeneration, ballooning of hepatocytes, nodular formation, and retained normal lobular architecture of hepatic parenchyma. It was observed that treatment with HPE reduced cell injury, inflammatory lesions, and restored hepatic lobular architecture in methotrexate induced hepatotoxicity in rats [41]. Placental extract can reduce liver interstitial collagen deposition, lipogenesis, inflammatory cell infiltration, and thus improve hepatic morphology and function [42]. Furthermore, it can prevent hepatocellular injury by scavenging ROS, inhibiting inflammatory cytokine production, blocking hepatocyte apoptosis and necrosis, and ultimately promote hepatocyte regeneration [42]. The regeneration of hepatocytes can rapidly replace the damaged and injured hepatocytes leading to the efficient functional recovery of the impaired liver.

The hepatic stellate cells, also known as perisinusoidal cells, are multifunctional nonparenchymal cells located in the space of Disse and are the most prominent cell type involved in the pathogenesis and progression of hepatic fibrosis [43]. The activation and transformation of round quiescent hepatic stellate cells into myofibroblast like cells with the expression of α-smooth muscle actin filaments is considered as the initial step in the pathogenesis of hepatic fibrosis [44]. The activation of stellate cells is a dynamic process accompanied with the production of various cytokines and growth factors and a major rate limiting event in the progression of hepatic fibrosis [45]. It is now well established that blocking the activation of hepatic stellate cells can arrest the pathogenesis of hepatic fibrosis and deposition of collagen fibers in the hepatic parenchyma [46]. In the present study, immunohistochemical staining demonstrated conspicuous and remarkable activation of stellate cells in the hepatic parenchyma of SHRSP5/Dmcr rats fed with HFC diet at 6, 8, and 12 W. Treatment with HPE resulted in a significant and marked reduction in the activation of stellate cells on all the days studied. It was reported that HPE treatment inhibits activation of hepatic stellate cells and ameliorates liver fibrosis in MCD-diet induced mouse model of MASH [36]. Furthermore, it was observed that porcine placental extract attenuated lipid peroxidation, suppressed TGF-β1 signaling, and reduced activation of

hepatic stellate cells in an animal model of MASH induced with HFC diet [47]. Placental extracts are abundant in anti-inflammatory cytokines, interleukin (IL)-1 receptor antagonist, IL-4, IL-10, IL-11, and IL-13 [42]. It also contains growth factors such as granulocyte-colony stimulating factor (G-CSF), granulocyte-macrophage colony stimulating factor (GM-CSF), epidermal growth factor (EGF), fibroblast growth factor (FGF), hepatocyte growth factor (HGF), insulin-like growth factor (IGF), platelet-derived growth factor (PDGF), transforming growth factor (TGF), and vascular endothelial growth factor (VEGF), which are involved in an array of physiological effects ranging from immunomodulation, anti-inflammatory, wound healing, cellular proliferation, and regeneration that make HPE a promising hepatoprotective agent [48].

The generation of free radicals, including a variety of ROS, leading to cellular oxidative stress and subsequent lipid peroxidation is a characteristic feature of MASH. Increased levels of serum MDA is an indication of elevated oxidative stress and membrane lipid peroxidation. Malondialdehyde is a final product of lipid peroxidation of polyunsaturated fatty acids and one of the best markers of cellular oxidative stress [49]. It was reported that HPE treatment reduced oxidative stress and MDA levels in the liver tissue after methotrexate-induced hepatotoxicity in rats [41]. In addition, treatment with Laennec (HPE) decreased hepatic MDA levels and nitric oxide in concanavalin-A induced liver injury in a murine model and indicated that Laennec has a protective effect against immune-mediated liver injury [50]. In the present study, HPE administration maintained normal levels of GSH and prevented increase in hepatic MDA levels. The potent antioxidant properties of HPE have been evaluated on random-pattern skin flap surgical wounds in rats and found significantly lower MDA and higher GSH levels in the group treated with HPE, suggesting HPE is a novel therapeutic agent for wound healing [51].

Increased oxidative stress and a marked decrease in the levels of antioxidants are common features in the pathogenesis of MASH and the accompanied hepatic fibrosis. In the present study, we observed a significant decrease in GSH levels at 8 and 12 W after the start of HFC diet in SHRSP5/Dmcr rats. We have also reported a remarkable decrease in the concentrations of the potent antioxidant ascorbic acid during the pathogenesis of N-nitrosodimethylamine induced hepatic fibrosis in rats [52]. Excessive formation of 4-hydroxy-2-nonenal (4-HNE) in the hepatic parenchyma is considered the most reliable biomarker for elevated oxidative stress and lipid peroxidation during liver injury [53]. The aldehyde, 4-HNE is a major end-product of the peroxidation of omega-6 unsaturated fatty acids such as linoleic acid and arachidonic acid [54]. In the present study, there was remarkable staining for 4-HNE, especially at 8 and 12 W in rats fed with HFC diet, indicating lipid peroxidation or oxidative degradation of membrane lipids. Treatment with HPE markedly reduced the staining intensity of 4-HNE on all the days evaluated, indicating the antioxidant potency of placental extract. It was reported that HPE treatment suppressed oxidative stress and significantly reduced 4-HNE in MCD diet-induced mouse model of MASH [55]. A collagen derived peptide with Glycine-XY amino acid repeats has been reported with the antioxidant activity associated with HPE and suggested that the oxidation of proline and hydroxyproline present in collagen might be involved in the antioxidant activity associated with collagen peptides [56]. Furthermore, it was observed that HPE treatment induced the production of anti-oxidase enzymes such as heme oxygenase-1 (HMOX1), NAD(P)H quinone dehydrogenase-1 (NQO1), catalase (CAT), and superoxide dismutase-1 (SOD1) in cultured hepatic stellate cells [36]. The current data and previous reports indicate that multiple components present in the HPE act simultaneously to suppress oxidative stress, reduce lipid peroxidation, and thus decrease cell injury.

Excessive synthesis and deposition of fibril forming collagens, predominantly type I and type III, in the extracellular matrix of the liver is the characteristic feature of hepatic fibrosis and liver cirrhosis [32,57]. We have demonstrated that during the pathogenesis and progression of hepatic fibrosis and early cirrhosis, the rate of synthesis and deposition of collagen type III is more prominent than that of collagen type I, and fibrotic liver collagen is more cross-linked than normal liver collagen [58]. In the current study, real-time quantitative PCR demonstrated a dramatic up-regulation in the expression of collagen type I and type III genes in the hepatic tissue of rats fed with HFC diet. Furthermore, immunohistochemical staining for collagen type I and type III depicted excessive synthesis and deposition of both collagen types in the hepatic parenchyma. The images demonstrated a well developed hepatic fibrosis at 8W and complete cirrhosis at 12W. Treatment with HPE markedly reduced the expression as well as deposition of both collagen types, prevented bridging fibrosis and nodular formation, and retained the normal lobular architecture of the liver. It was reported that HPE treatment effectively ameliorated liver fibrosis in MASH due to suppression of the activation of hepatic stellate cells [36]. Overall, the current data and previous reports strongly suggest that HPE is a natural medicine with potent therapeutic effects and could suppress fatty degeneration and MASH, regress liver injury, prevent progression of hepatic fibrosis to cirrhosis, and may block related adverse events such as HCC. The mechanisms of the therapeutic effect of HPE may be attributed to antioxidant, anti-inflammatory, anti-apoptosis, immunotropic, and the ability to promote hepatocyte regeneration. However, HPE treatment may not be effective to reverse advanced stages of MASH with hepatic fibrosis.

Clinical Science (2024) **138** 327–349
https://doi.org/10.1042/CS20230533

Conclusions

The results of the present study demonstrated that administration of HPE remarkably reduces HFC diet induced pathogenesis of MASH and the associated development of severe hepatic fibrosis and early cirrhosis in an experimental animal model. The data indicate that HPE treatment mediates immunotropic, anti-inflammatory, and antioxidant responses, attenuates fatty degeneration, and inhibits the pathogenesis of hepatic fibrosis and early cirrhosis. HPE shows as a therapeutic agent to inhibit the progression of MASH and the associated hepatic fibrosis towards liver cirrhosis.

Clinical perspectives

- Evaluate the effects of human placental extract (HPE) to attenuate experimentally induced steatotic liver disease (SLD) and hepatic fibrosis.
- Treatment with HPE improved liver functions, reduced excessive deposition of fat in the liver, and markedly attenuated SLD and hepatic fibrosis.
- HPE shows promise as a therapeutic agent to prevent progression of MASH to liver cirrhosis.

Data Availability

The data will be available for verification upon request.

Competing Interests

The authors declare that there are no competing interests associated with the manuscript.

Funding

This research work was supported by Grant from Kanazawa Medical University [grant number RP 2017-05 (to M.T.)].

CRediT Author Contribution

Mitsuyoshi Yamagata: Resources, Data curation, Formal analysis, Investigation. **Mutsumi Tsuchishima:** Conceptualization, Resources, Supervision. **Takashi Saito:** Software, Formal analysis, Validation, Visualization. **Mikihiro Tsutsumi:** Conceptualization, Supervision, Funding acquisition, Writing—original draft, Project administration. **Joseph George:** Supervision, Validation, Methodology, Writing—original draft, Writing—review & editing.

Ethics Approval

The animal experiments were carried out as per the Guide for the Care and Use of Laboratory Animals published by the US National Institutes of Health (NIH Publication No. 86-23, revised 1996). The animal experimental protocol was approved by the Animal Care and Use Committee of Kanazawa Medical University on the Ethics of use and care of experimental animals (#2018−29).

Acknowledgements

The authors are thankful to Mr Mitsuru Araya for his excellent technical assistance and support in the laboratory work and animal experiments. The authors express their gratitude to Dr Atsushi Fukumura for critical reading of the manuscript.

Abbreviations

α-SMA, α-smooth muscle actin; 4-HNE, 4-hydroxy-2-nonenal; AEC, 3-amino-9-ethylcarbazole; ALT, alanine aminotransferase; AST, aspartate aminotransferase; CAT, catalase; DMCR, Disease Models Co-operative research; EDTA, ethylene diamine tetraacetic acid; EGF, epidermal growth factor; FGF, fibroblast growth factor; GAPDH, glyceraldehyde 3-phosphate dehydrogenase; G-CSF, granulocyte-colony stimulating factor; GM-CSF, granulocyte-macrophage colony stimulating factor; GSH, reduced glutathione; H&E, Hematoxylin and Eosin; HBV, Hepatitis B virus; HCC, hepatocellular carcinoma; HCV, Hepatitis C virus; HFC diet, high-fat and high-cholesterol diet; HGF, hepatocyte growth factor; HIV, human immunodeficiency virus; HMOX1, heme oxygenase 1; HPE, human placental extract; HPV, human papillomavirus; HSV, Herpes simplex virus; IGF, insulin-like growth factor; IL, interleukin; MASH, metabolic dysfunction-associated steatohepatitis; MASLD, metabolic dysfunction-associated steatotic liver disease; MCD, methionine and choline deficient; MDA, malondialdehyde; NDMA, N-nitrosodimethylamine; NQO1,

NAD(P)H quinone dehydrogenase 1; PCNA, proliferating cell nuclear antigen; PDGF, platelet-derived growth factor; qPCR, quantitative polymerase chain reaction; ROS, reactive oxygen species; SAF score, steatosis, activity, fibrosis score; SHRSP, stroke-prone spontaneously hypertensive rat; SLD, steatotic liver disease; SOD1, superoxide dismutase 1; SPs, stroke-prone; SYBR Green, Synergy brands green; TGF, transforming growth factor; VEGF, vascular endothelial growth factor.

References

1 Sanyal, A.J., Van Natta, M.L., Clark, J., Neuschwander-Tetri, B.A., Diehl, A., Dasarathy, S. et al. (2021) NASH Clinical Research Network (CRN). Prospective study of outcomes in adults with nonalcoholic fatty liver disease. *N. Engl. J. Med.* **385**, 1559–1569, https://doi.org/10.1056/NEJMoa2029349
2 Rinella, M.E., Lazarus, J.V., Ratziu, V., Francque, S.M., Sanyal, A.J., Kanwal, F. et al. (2023) A multisociety Delphi consensus statement on new fatty liver disease nomenclature. *J. Hepatol.* **79**, 1542–1556, https://doi.org/10.1016/j.jhep.2023.06.003
3 Chan, W.K., Chuah, K.H., Rajaram, R.B., Lim, L.L., Ratnasingam, J. and Vethakkan, S.R. (2023) Metabolic dysfunction-associated steatotic liver disease (MASLD): a state-of-the-art review. *J. Obes. Metab. Syndr.* **32**, 197–213, https://doi.org/10.7570/jomes23052
4 Takahashi, Y., Dungubat, E., Kusano, H. and Fukusato, T. (2023) Pathology and pathogenesis of metabolic dysfunction-associated steatotic liver disease-associated hepatic tumors. *Biomedicines* **11**, 2761, https://doi.org/10.3390/biomedicines11102761
5 Anstee, Q.M., McPherson, S. and Day, C.P. (2011) How big a problem is non-alcoholic fatty liver disease? *BMJ* **343**, d3897, https://doi.org/10.1136/bmj.d3897
6 Ratziu, V., Bellentani, S., Cortez-Pinto, H., Day, C. and Marchesini, G. (2010) A position statement on NAFLD/NASH based on the EASL 2009 special conference. *J. Hepatol.* **53**, 372–384, https://doi.org/10.1016/j.jhep.2010.04.008
7 Kothari, S., Dhami-Shah, H. and Shah, S.R. (2019) Antidiabetic drugs and statins in nonalcoholic fatty liver disease. *J. Clin. Exp. Hepatol.* **9**, 723–730, https://doi.org/10.1016/j.jceh.2019.06.003
8 Dite, P., Blaho, M., Bojkova, M., Jabandziev, P. and Kunovsky, L. (2020) Nonalcoholic fatty pancreas disease: clinical consequences. *Dig. Dis.* **38**, 143–149, https://doi.org/10.1159/000505366
9 Khan, R.S. and Newsome, P.N. (2016) Non-alcoholic fatty liver disease and liver transplantation. *Metabolism* **65**, 1208–1223, https://doi.org/10.1016/j.metabol.2016.02.013
10 Kubota, R., Hayashi, N., Kinoshita, K., Saito, T., Ozaki, K., Ueda, Y. et al. (2020) Inhibition of γ-glutamyltransferase ameliorates ischaemia-reoxygenation tissue damage in rats with hepatic steatosis. *Br. J. Pharmacol.* **177**, 5195–5207, https://doi.org/10.1111/bph.15258
11 Esquivel, C.O. (2010) Liver transplantation: where we are and where we are heading. *Transplant. Proc.* **42**, 610–612, https://doi.org/10.1016/j.transproceed.2010.02.013
12 Emara, A.K., Anis, H. and Piuzzi, N.S. (2020) Human placental extract: the feasibility of translation from basic science into clinical practice. *Ann. Transl. Med.* **8**, 156, https://doi.org/10.21037/atm.2020.01.50
13 Sur, T.K., Biswas, T.K., Ali, L. and Mukherjee, B. (2003) Anti-inflammatory and anti-platelet aggregation activity of human placental extract. *Acta Pharmacol. Sin.* **24**, 187–192
14 Kwon, T.R., Oh, C.T., Park, H.M., Han, H.J., Ji, H.J. and Kim, B.J. (2015) Potential synergistic effects of human placental extract and minoxidil on hair growth-promoting activity in C57BL/6J mice. *Clin. Exp. Dermatol.* **40**, 672–681, https://doi.org/10.1111/ced.12601
15 Parolini, O. and Caruso, M. (2011) Review: Preclinical studies on placenta-derived cells and amniotic membrane: an update. *Placenta* **32**, S186–S195, https://doi.org/10.1016/j.placenta.2010.12.016
16 Pogozhykh, O., Prokopyuk, V., Figueiredo, C. and Pogozhykh, D. (2018) Placenta and placental derivatives in regenerative therapies: Experimental studies, history, and prospects. *Stem Cells Int.* **2018**, 4837930, https://doi.org/10.1155/2018/4837930
17 Samiei, F., Jamshidzadeh, A., Noorafshan, A. and Ghaderi, A. (2016) Human placental extract ameliorates structural lung changes induced by amiodarone in rats. *Iran J. Pharm. Res.* **15**, 75–82
18 Rozanova, S. (2014) Antioxidant properties of extracts derived from placentae of different gestation terms. *Oxid. Antioxid. Med. Sci.* **3**, 181–186, https://doi.org/10.5455/oams.070914.or.073
19 Qanungo, S. and Mukherjea, M. (2000) Ontogenic profile of some antioxidants and lipid peroxidation in human placental and fetal tissues. *Mol. Cell. Biochem.* **215**, 11–19, https://doi.org/10.1023/A:1026511420505
20 Mohamed, N.S., Wilkie, W.A., Remily, E.A. and Delanois, R.E. (2020) Can human placental extract help patients with osteoarthritis? *Ann. Transl. Med.* **8**, 62, https://doi.org/10.21037/atm.2019.12.135
21 Lee, K.H., Kim, T.H., Lee, W.C., Kim, S.H., Lee, S.Y. and Lee, S.M. (2011) Anti-inflammatory and analgesic effects of human placenta extract. *Nat. Prod. Res.* **25**, 1090–1100, https://doi.org/10.1080/14786419.2010.489050
22 Choi, J.Y., Lee, K., Lee, S.M., Yoo, S.H., Hwang, S.G., Choi, J.Y. et al. (2014) Efficacy and safety of human placental extract for alcoholic and nonalcoholic steatohepatitis: an open-label, randomized, comparative study. *Biol. Pharm. Bull.* **37**, 1853–1859, https://doi.org/10.1248/bpb.b13-00979
23 Park, S.Y., Phark, S., Lee, M., Lim, J.Y. and Sul, D. (2010) Anti-oxidative and anti-inflammatory activities of placental extracts in benzo[a]pyrene-exposed rats. *Placenta* **31**, 873–879, https://doi.org/10.1016/j.placenta.2010.07.010
24 Kitamori, K., Naito, H., Tamada, H., Kobayashi, M., Miyazawa, D., Yasui, Y. et al. (2012) Development of novel rat model for high-fat and high-cholesterol diet-induced steatohepatitis and severe fibrosis progression in SHRSP5/Dmcr. *Environ. Health Prev. Med.* **17**, 173–182, https://doi.org/10.1007/s12199-011-0235-9
25 Watanabe, S., Kumazaki, S., Yamamoto, S., Sato, I., Kitamori, K., Mori, M. et al. (2018) Non-alcoholic steatohepatitis aggravates nitric oxide synthase inhibition-induced arteriosclerosis in SHRSP5/Dmcr rat model. *Int. J. Exp. Pathol.* **99**, 282–294, https://doi.org/10.1111/iep.12301

Clinical Science (2024) **138** 327–349
https://doi.org/10.1042/CS20230533

26 George, J. and Chandrakasan, G. (2000) Biochemical abnormalities during the progression of hepatic fibrosis induced by dimethylnitrosamine. *Clin. Biochem.* **33**, 563–570, https://doi.org/10.1016/S0009-9120(00)00170-3

27 Bedossa, P., Poitou, C., Veyrie, N., Bouillot, J.L., Basdevant, A., Paradis, V. et al. (2012) Histopathological algorithm and scoring system for evaluation of liver lesions in morbidly obese patients. *Hepatology* **56**, 1751–1759, https://doi.org/10.1002/hep.25889

28 Nomura, M., George, J., Hashizume, C., Saito, T., Ueda, Y., Ishigaki, Y. et al. (2022) Surgical implantation of human adipose derived stem cells attenuates experimentally induced hepatic fibrosis in rats. *Mol. Med.* **28**, 143, https://doi.org/10.1186/s10020-022-00566-6

29 George, J., Tsuchishima, M. and Tsutsumi, M. (2022) Epigallocatechin-3-gallate inhibits osteopontin expression and prevents experimentally induced hepatic fibrosis. *Biomed. Pharmacother.* **151**, 113111, https://doi.org/10.1016/j.biopha.2022.113111

30 George, J., Tsuchishima, M. and Tsutsumi, M. (2020) Metabolism of N-nitrosodimethylamine, methylation of macromolecules, and development of hepatic fibrosis in rodent models. *J. Mol. Med. (Berl.)* **98**, 1203–1213, https://doi.org/10.1007/s00109-020-01950-7

31 George, J., Tsutsumi, M. and Tsuchishima, M. (2019) Alteration of trace elements during pathogenesis of *N*-Nitrosodimethylamine induced hepatic fibrosis. *Sci. Rep.* **9**, 708, https://doi.org/10.1038/s41598-018-37516-4

32 Minato, T., Tsutsumi, M., Tsuchishima, M., Hayashi, N., Saito, T., Matsue, Y. et al. (2014) Binge alcohol consumption aggravates oxidative stress and promotes pathogenesis of NASH from obesity-induced simple steatosis. *Mol. Med.* **20**, 490–502, https://doi.org/10.2119/molmed.2014.00048

33 George, J., Rao, K.R., Stern, R. and Chandrakasan, G. (2001) Dimethylnitrosamine-induced liver injury in rats: the early deposition of collagen. *Toxicology* **156**, 129–138, https://doi.org/10.1016/S0300-483X(00)00352-8

34 Jiang, C.M., Pu, C.W., Hou, Y.H., Chen, Z., Alanazy, M. and Hebbard, L. (2014) Non alcoholic steatohepatitis a precursor for hepatocellular carcinoma development. *World J. Gastroenterol.* **20**, 16464–16473, https://doi.org/10.3748/wjg.v20.i44.16464

35 George, J., Tsuchishima, M. and Tsutsumi, M. (2019) Molecular mechanisms in the pathogenesis of N-nitrosodimethylamine induced hepatic fibrosis. *Cell Death Dis.* **10**, 18, https://doi.org/10.1038/s41419-018-1272-8

36 Yamauchi, A., Tone, T., Toledo, A., Igarashi, K., Sugimoto, K., Miyai, H. et al. (2020) Placental extract ameliorates liver fibrosis in a methionine- and choline-deficient diet-induced mouse model of non-alcoholic steatohepatitis. *Biomed. Res.* **41**, 1–12, https://doi.org/10.2220/biomedres.41.1

37 Jung, J., Lee, H.J., Lee, J.M., Na, K.H., Hwang, S.G. and Kim, G.J. (2011) Placenta extract promote liver regeneration in CCl_4-injured liver rat model. *Int. Immunopharmacol.* **11**, 976–984, https://doi.org/10.1016/j.intimp.2011.02.012

38 Shimokobe, H., Sumida, Y., Tanaka, S., Mori, K., Kitamura, Y., Fukumoto, K. et al. (2015) Human placental extract treatment for non-alcoholic steatohepatitis non-responsive to lifestyle intervention: A pilot study. *Hepatol. Res.* **45**, 1034–1040, https://doi.org/10.1111/hepr.12432

39 George, J. and Chandrakasan, G. (1996) Glycoprotein metabolism in dimethylnitrosamine induced hepatic fibrosis in rats. *Int. J. Biochem. Cell Biol.* **28**, 353–361, https://doi.org/10.1016/1357-2725(95)00140-9

40 Liu, K.X., Kato, Y., Kaku, T. and Sugiyama, Y. (1998) Human placental extract stimulates liver regeneration in rats. *Biol. Pharm. Bull.* **21**, 44–49, https://doi.org/10.1248/bpb.21.44

41 Ghoneum, M. and El-Gerbed, M.S.A. (2021) Human placental extract ameliorates methotrexate-induced hepatotoxicity in rats via regulating antioxidative and anti-inflammatory responses. *Cancer Chemother. Pharmacol.* **88**, 961–971, https://doi.org/10.1007/s00280-021-04349-4

42 Shen, L.H., Fan, L., Zhang, Y., Zhu, Y.K., Zong, X.L., Peng, G.N. et al. (2022) Protective effect and mechanism of placenta extract on liver. *Nutrients* **14**, 5071, https://doi.org/10.3390/nu14235071

43 Shang, L., Hosseini, M., Liu, X., Kisseleva, T. and Brenner, D.A. (2018) Human hepatic stellate cell isolation and characterization. *J. Gastroenterol.* **53**, 6–17, https://doi.org/10.1007/s00535-017-1404-4

44 George, J. (2018) Determination of selenium during pathogenesis of hepatic fibrosis employing hydride generation and inductively coupled plasma mass spectrometry. *Biol. Chem.* **399**, 499–509, https://doi.org/10.1515/hsz-2017-0260

45 George, J., Tsutsumi, M. and Takase, S. (2004) Expression of hyaluronic acid in N-nitrosodimethylamine induced hepatic fibrosis in rats. *Int. J. Biochem. Cell Biol.* **36**, 307–319, https://doi.org/10.1016/S1357-2725(03)00253-X

46 George, J., Tsutsumi, M. and Tsuchishima, M. (2017) MMP-13 deletion decreases profibrogenic molecules and attenuates N-nitrosodimethylamine-induced liver injury and fibrosis in mice. *J. Cell. Mol. Med.* **21**, 3821–3835, https://doi.org/10.1111/jcmm.13304

47 Xu, L., Nagata, N., Nagashimada, M., Zhuge, F., Ni, Y., Chen, G. et al. (2018) A porcine placental extract prevents steatohepatitis by suppressing activation of macrophages and stellate cells in mice. *Oncotarget* **9**, 15047–15060, https://doi.org/10.18632/oncotarget.24587

48 Pan, S.Y., Chan, M.K.S., Wong, M.B.F., Klokol, D. and Chernykh, V. (2017) Placental therapy: An insight to their biological and therapeutic properties. *J. Med. Therap.* **1**, 1–6

49 Vuppalanchi, R., Juluri, R., Bell, L.N., Ghabril, M., Kamendulis, L., Klaunig, J.E. et al. (2011) Oxidative stress in chronic liver disease: relationship between peripheral and hepatic measurements. *Am. J. Med. Sci.* **342**, 314–317, https://doi.org/10.1097/MAJ.0b013e31821d9905

50 Wu, J., Yang, T., Wang, C., Liu, Q., Yao, J., Sun, H. et al. (2008) Laennec protects murine from concanavalin A-induced liver injury through inhibition of inflammatory reactions and hepatocyte apoptosis. *Biol. Pharm. Bull.* **31**, 2040–2044, https://doi.org/10.1248/bpb.31.2040

51 Kwon, J.W., Hong, S.E., Kang, S.R. and Park, B.Y. (2019) Effect of human placental extract treatment on random-pattern skin flap survival in rats. *J. Invest. Surg.* **32**, 304–313, https://doi.org/10.1080/08941939.2017.1417518

52 George, J. (2003) Ascorbic acid concentrations in dimethylnitrosamine-induced hepatic fibrosis in rats. *Clin. Chim. Acta* **335**, 39–47, https://doi.org/10.1016/S0009-8981(03)00285-7

53 Poli, G., Biasi, F. and Leonarduzzi, G. (2008) 4-Hydroxynonenal-protein adducts: A reliable biomarker of lipid oxidation in liver diseases. *Mol. Aspects Med.* **29**, 67–71, https://doi.org/10.1016/j.mam.2007.09.016

54 Ayala, A., Muñoz, M.F. and Argüelles, S. (2014) Lipid peroxidation: production, metabolism, and signaling mechanisms of malondialdehyde and 4-hydroxy-2-nonenal. *Oxid. Med. Cell Longev.* **2014**, 360438, https://doi.org/10.1155/2014/360438

55 Yamauchi, A., Kamiyoshi, A., Koyama, T., Iinuma, N., Yamaguchi, S., Miyazaki, H. et al. (2017) Placental extract ameliorates non-alcoholic steatohepatitis (NASH) by exerting protective effects on endothelial cells. *Heliyon* **3**, e00416, https://doi.org/10.1016/j.heliyon.2017.e00416

56 Togashi, S., Takahashi, N., Iwama, M., Watanabe, S., Tamagawa, K. and Fukui, T. (2002) Antioxidative collagen-derived peptides in human-placenta extract. *Placenta* **23**, 497–502, https://doi.org/10.1053/plac.2002.0833
57 George, J. (2008) Elevated serum beta-glucuronidase reflects hepatic lysosomal fragility following toxic liver injury in rats. *Biochem. Cell Biol.* **86**, 235–243, https://doi.org/10.1139/008-038
58 George, J. and Chandrakasan, G. (1996) Molecular characteristics of dimethylnitrosamine induced fibrotic liver collagen. *Biochim. Biophys. Acta* **1292**, 215–222, https://doi.org/10.1016/0167-4838(95)00202-2